Increasing solar reflectivity of building envelope materials to mitigate urban heat islands: state-of-the-art review

Ziaeemehr, Bahador; Jandaghian, Zahra; Ge, Hua; Lacasse, Michael Lacasse; Moore, Travis

Publisher's version / Version de l'éditeur:
https://doi.org/10.3390/buildings13112868
Buildings, 13, 11, 2023-11-16

buildings

MDPI

Review

Increasing Solar Reflectivity of Building Envelope Materials to Mitigate Urban Heat Islands: State-of-the-Art Review

Bahador Ziaeemehr [1], Zahra Jandaghian [2,*], Hua Ge [1], Michael Lacasse [2] and Travis Moore [2]

[1] Department of Building, Civil & Environmental Engineering, Concordia University, Montreal, QC H3G 1M8, Canada; bahador.ziaeemehr@concordia.ca (B.Z.)
[2] Construction Research Centre, National Research Council Canada, Ottawa, ON K1A 0R6, Canada
* Correspondence: zahra.jandaghian@nrc-cnrc.gc.ca

Abstract: The Urban Heat Island (UHI), a consequence of urban development, leads to elevated temperatures within cities compared to their rural counterparts. This phenomenon results from factors such as urban designs, anthropogenic heat emissions, and materials that absorb and retain solar radiation in the built environment. Materials commonly used in cities, like concrete, asphalt, and stone, capture solar energy and subsequently emit it as heat into the surroundings. Consequently, this phenomenon amplifies summertime cooling energy demands in buildings. To mitigate the UHI impacts, various mitigation strategies have emerged that include but are not limited to using higher solar reflectivity materials, known as "cool materials", and increasing vegetation and greenery in urban areas. Cool materials have high reflectivity and emissivity, effectively reflecting solar radiation while emitting absorbed heat through radiative cooling. Increasing the solar reflectivity of building envelope materials is a promising sustainable solution to lessen the UHI effects. This state-of-the-art review summarizes the UHI causes and effects, states the mitigation strategies, describes the cool building envelope materials, explains the solar reflectivity index measurements, indicates the building and micro-climate simulations, highlights the performance evaluation of using cool building envelope materials, points out the research gaps, and proposes future research opportunities.

Keywords: urban heat island (UHI); solar reflectivity index; solar emissivity; building envelope materials; cool materials

Citation: Ziaeemehr, B.; Jandaghian, Z.; Ge, H.; Lacasse, M.; Moore, T. Increasing Solar Reflectivity of Building Envelope Materials to Mitigate Urban Heat Islands: State-of-the-Art Review. *Buildings* **2023**, *13*, 2868. https://doi.org/10.3390/buildings13112868

Academic Editor: Geun Young Yun

Received: 15 September 2023
Revised: 30 October 2023
Accepted: 12 November 2023
Published: 16 November 2023

1. Introduction

The Urban Heat Island (UHI) is characterized by localized surface and air temperature elevations in dense urban areas, resulting from a complex interplay of changes in land use/land cover, thermal characteristics of urban materials, and heat generated by human activities due to increased energy consumption. The UHI degrades the comfort and well-being of urban inhabitants, increases energy demands, exacerbates air pollution, and augments greenhouse gas emissions.

In response to this challenge, researchers have been seeking effective mitigation and adaptation strategies to counteract its adverse effects. The UHI mitigation techniques include but are not limited to using materials with higher solar reflectivity and planting more vegetation in urban communities. This paper provides a comprehensive literature review on using materials with higher solar reflectivity and higher heat emissivity, known as "cool materials". Figure 1 presents the roadmap that this manuscript focuses on. These so-called cool materials reflect solar radiation to the atmosphere and dissipate absorbed heat through the emission of thermal radiation, resulting in cooler surface and air temperatures.

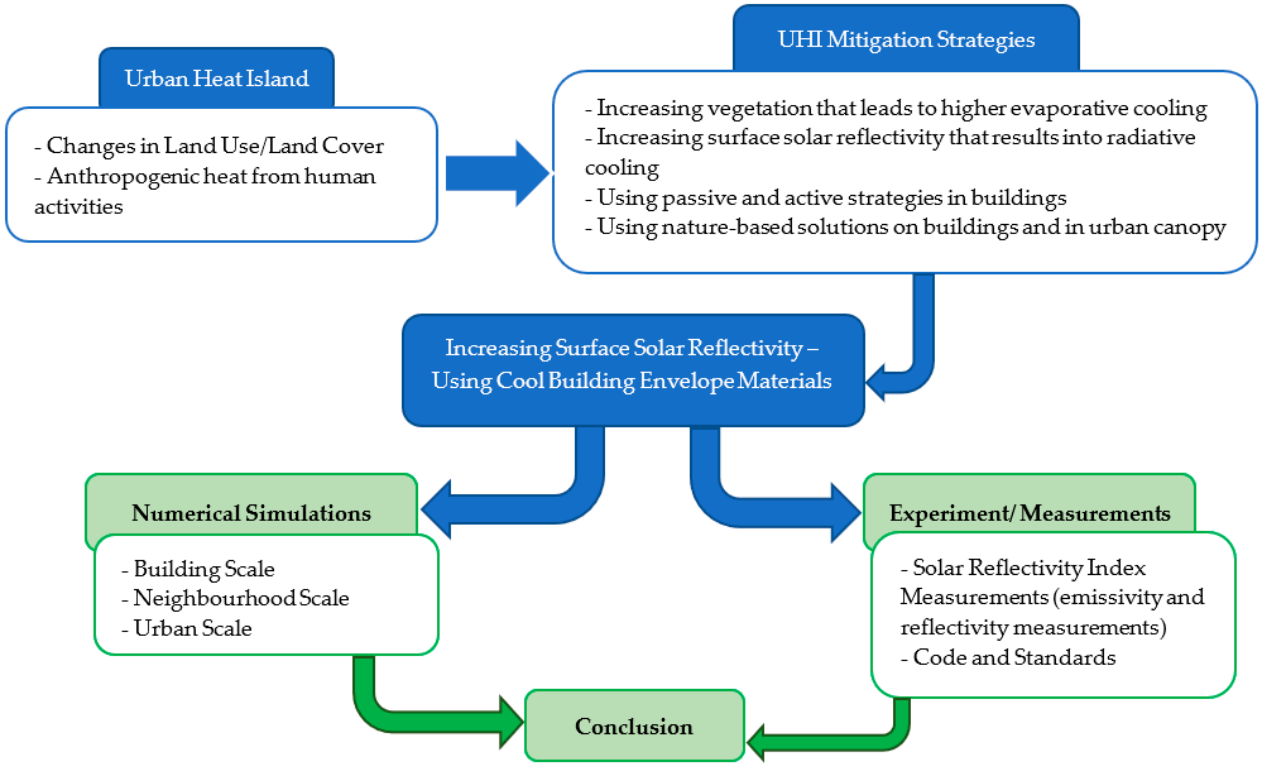

Figure 1. Roadmap presenting the focus of this manuscript.

Urban infrastructure, solar radiation, absorptive building materials, and anthropogenic heat emission, combined with reduced natural cooling processes, create a complex and interconnected system of urban heat sources that lead to the UHI phenomenon. Understanding and managing these sources are crucial steps in developing effective strategies to mitigate the adverse effects on human health, energy use, and urban climate.

2. UHI Causes and Effects

Introduced by Howard in 1818 [1], the UHI effect is a well-known consequence of urban development, resulting in elevated temperatures within urban areas when compared to the adjacent rural regions (Figure 2). It is primarily caused by factors such as building shapes, structures, and materials that capture and retain solar radiation during daylight hours. At night, urban areas experience reduced loss of radiation due to narrower street canyons and limited cooling potential through evaporation [2]. The UHI effect leads to an increased demand for summertime cooling energy in buildings and, conversely, a decreased demand for heating energy during the cold season [3]. The UHI effect intensifies heat waves, hindering nighttime cooling in buildings and thereby affecting human well-being. Effective strategies to mitigate the UHI impacts consider the interaction of various microclimates and building types to comprehensively address the urban climate [4]. Due to the rise in urban temperatures and the occurrence of extreme heat waves, there is a heightened probability of overheating events taking place in buildings.

The first contributors to UHI are factors that control energy balance at the Earth's surface. These factors include incoming solar radiation, solar radiation absorbed and reflected by the atmosphere, infrared radiation emitted by the Earth, and infrared radiation absorbed and re-emitted by the atmosphere, primarily due to greenhouse gases. These factors interact through complex physical processes and play a role in shaping the Earth's climate, including temperature, precipitation, wind patterns, humidity, and other variables. Approximately 30% of the incoming shortwave radiation from the sun is reflected into space, whereas the remaining portion is absorbed by the Earth's system. The fraction of solar radiation scattered back to the atmosphere depends on the reflectivity (albedo) of

various components such as clouds, land surfaces (including snow and ice), oceans, and atmospheric particles (aerosols). Cloud, snow, and ice cover have a particularly strong influence on the amount of solar radiation reflected due to their higher albedo compared to land and oceans [5].

Figure 2. Urban areas experience higher surface and air temperatures than their surrounding rural areas due to changes in land use/land cover and human activities [5].

Therefore, the solar radiation that is absorbed and retained by various surfaces in the urban landscape, such as buildings, roads, and pavements, plays a role in the UHI phenomenon [3]. The main source of thermal load at the building's outer surface is incident solar radiation. The amount of irradiation resulting from direct solar radiation is contingent on the angle between the sun and the exposed surface and on the surface's short-wave absorptivity [5]. Hence, estimating heat gain from solar radiation on a building envelope involves considering multiple factors, including solar radiation intensity, building orientation, window area and orientation, presence of shading devices, solar heat gain coefficient, and consideration of thermal properties of materials [5].

The second contributor to UHI is anthropogenic heat generated by human activities in cities. This includes heat emissions from buildings, industrial processes, transportation, and energy-conversion processes [3]. Anthropogenic heat sources can trigger a feedback loop, elevating outdoor temperatures and increasing building cooling demand to permit maintaining indoor comfort [6], which in return results in increased anthropogenic heat generation. Furthermore, industrial processes, power plants, and other energy generation sources emit waste heat, which is discharged into the urban surroundings. This surplus heat can substantially augment the overall thermal burden in urban areas [3]. It is imperative to conduct further research encompassing different climatic conditions to fully evaluate the heat emission sources and their effects on mitigation strategies.

In addition, materials used in urban infrastructure, such as concrete, asphalt, and stone, can absorb and retain heat, thereby contributing to UHI effects. These surfaces have a low albedo (reflectivity), which means they absorb more solar radiation converted into heat [3]. The urban form, defined by building characteristics and infrastructure, influences complex interactions within cities. Impacting factors are heat storage, wind patterns, and precipitation [6]. Materials commonly used in urban areas, such as concrete and asphalt, exhibit lower reflectivity (albedo), leading to reduced reflection of radiation. Moreover, these materials possess higher heat capacity, enabling them to retain more absorbed solar energy [7,8]. Also, lowering vegetation causes a reduction in the cooling effect achieved through evapotranspiration [9,10].

These factors combined result in a significant absorption and retention of heat within the urban environment. As a result, temperatures rise at a much faster rate compared to more natural areas [11]. The function, form, practical purposes, and contribution to the visual aspects of urban materials collectively influence UHI effects, while the usage and structure of urban spaces affect the energy budget and the timing of the UHI phenomenon. Diverse urban settings and canopies lead to varying occupancy and energy use, with industrial and air conditioning heat emissions directly affecting the urban environment's energy balance and leading to higher surface and ambient temperatures [12,13].

Consequently, the number of heat-related mortalities are magnified in urban regions [14]. Vulnerable populations to heat stress encompass older individuals (aged 65+), children (under 15), those with pre-existing health conditions or medications affecting thermoregulation, individuals of low socioeconomic status, and physically active individuals engaged in outdoor activities [15]. Urban heat waves pose a major risk to the general public's health and welfare. Many of the heat-related morbidity and mortality cases are caused by excessive indoor heating in long-term care home facilities, social housing, and buildings with elderly people inhabitants [16].

Considering most people spend the majority of time indoors necessitates accurate calculation and assurance of thermal comfort. Throughout history, the assessment of thermal comfort has posed challenges, with studies highlighting a disparity between perceived comfort and actual sensation. Recent research has focused primarily on the physiological responses to psychological disturbances, neglecting the critical factor of people's emotional states. In this context, the impact of occupants' mood states on thermal sensation was investigated by Turhan et al., and a novel element, the "Mood State Correction Factor", is introduced. This factor is intended to address the influence of occupants' moods on their perceived thermal comfort, ultimately aiming to provide a comprehensive and accurate assessment [17].

3. UHI Mitigation Strategies

Numerous approaches have been suggested to mitigate the adverse impacts of climate change and the Urban Heat Island (UHI) effects on buildings, inhabitants, pedestrian comfort, and the urban climate. [18]. However, achieving an optimal mitigation effect is challenging due to the intricate interactions among multiple elements, including weather patterns, urban texture (land use, building density, scale of building, street pattern, etc.), natural landscapes, ventilation, building energy consumption, and other elements. Consequently, the effectiveness of mitigation efforts should not be confined to singular aspects; rather, a more coherent and integrated approach is imperative to devise comprehensive heat mitigation solutions. Therefore, a thorough examination of each facet becomes essential to establishing well-rounded and effective heat mitigation measures [18].

In mitigation strategies, changes made to conditions directly affecting a building or person, like heat transfer and radiation, are called "direct effects". On the other hand, actions that adjust the conditions around a building or person are termed "indirect effects" [19]. Increasing solar reflectivity on roofing materials is one method that contributes to lowering the UHI effects [20]. However, studies show that the use of high-albedo roofs might result in a winter heating penalty due to reduced absorbed radiation, but this impact is minimal and depends on various factors and requires further investigation for different climatic zones [18,21,22]. During winter, roofs can be naturally covered by snow. Snow has a high albedo, meaning it reflects sunlight effectively. Consequently, any heating penalties experienced are not directly attributable to the cool roof itself but rather to the presence of snow, which contributes significantly to the solar reflection process [23].

In this paper, the focus is on increasing the surface solar reflectivity of buildings to directly and indirectly mitigate the UHI impacts. Enhancing surface reflectivity, as shown in Figure 3, can lower ambient temperatures, leading to decreased rates of photochemical reactions, reduced cooling energy requirements, and, consequently, enhanced air quality and human health [24]. High-albedo materials, reflecting solar radiation, can effectively reduce surface and air temperatures [25]. Table 1 shows the effects of increasing surface solar reflectivity on reducing surface and ambient temperatures in various climatic zones.

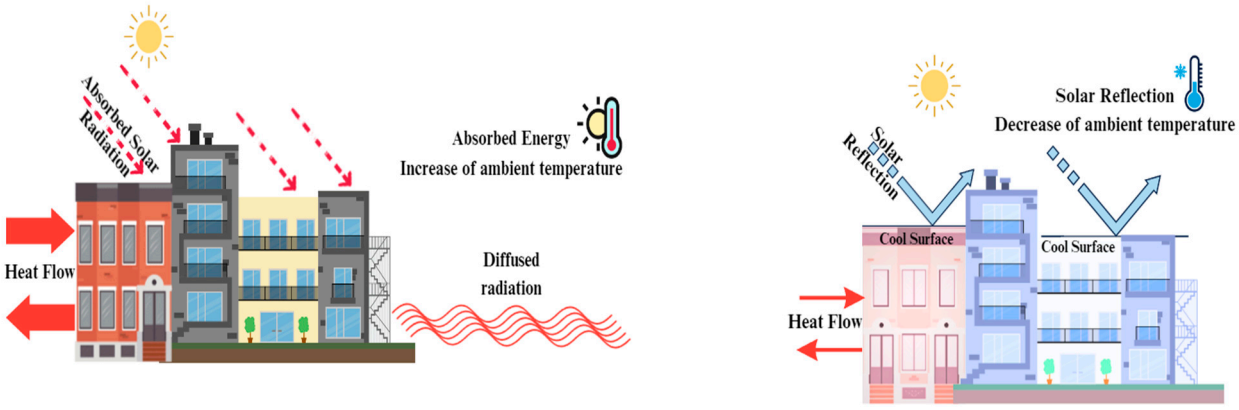

Figure 3. Increasing surface reflectivity in urban areas has the effect of reducing ambient temperatures. Absorbed energy refers to the quantity of solar radiation that is converted into heat and retained by the roof materials, whereas solar reflection pertains to the radiation that is reflected in the sky [5].

Table 1. Relationship between increased reflectivity and temperature reduction.

	City	Increasing Solar Reflectivity (ISR)	Temperature Reduction	Reference
1	Toronto, Canada	ISR on roofs, walls, and ground to 0.65, 0.60, and 0.45, respectively, from 0.2.	2 °C	[24]
2	Guangzhou, China	Cool coating, from 0.16–0.19 to 0.26–0.34	1–2.1 °C	[26]
3	United Arab Emirates	50% increase in surface reflectivity	22% decrease in surface temperature	[27]
4	Los Angeles, USA	ISR on roof to 0.35	3 °C	[28]
5	10 urbans, USA	ISR values increased by 0.30 on residential roofs and by 0.45 on office roofs.	1–2 °C	[29]
6	27 cities; Mediterranean, humid continental, subtropical arid, and desert conditions	ISR on roofs by 0.65	1.2–3.78 °C	[30]
7	Worldwide simulation	ISR on roofs to 0.9	0.3–0.6 °C	[31]
8	Mediterranean coastal area, Italy	ISR on urban surfaces from 0.3 to 0.55	2 °C	[32]
9	Melbourne, Australia	ISR on roofs from 0.50 to 0.85	2.2–5.2 °C	[33]
10	Midland, UK	ISR on roofs from 20% to 70%	0.3 °C	[34]
11	Jerusalem, Israel	ISR from 0.2 to 0.8	0.4 °C	[35]
12	Melbourne, Australia	ISR on urban surfaces to 0.27	0.9–1.6 °C	[36]

Table 2 and Figure 4 show a relationship between the reflective properties of materials and their influence on surface temperatures. Materials with higher solar reflectivity, such as light-colored or reflective coatings, effectively bounce back a significant portion of incoming solar radiation, reducing heat absorption and thus lowering surface temperatures. This data underscores the pivotal role that solar reflectivity plays in mitigating the UHI effect and advancing energy-efficient building design.

Table 2. Solar reflectance, emittance, and surface temperature for different roofing materials [37].

Roofing Materials	Solar Reflectance %	Temperature (°C)	Infrared Emittance %
Bitumen–smooth surface	6	46.1	86
Asphalt shingles—black granules	5	45.6	91
Built-up roof—dark gravel	12	42.2	90
Asphalt shingles—white granules	25	35.6	91
Bitumen–white granules	26	35	92
Built-up roof—light gravel	34	31.7	90
Shingles—white elastomeric coating	71	12.2	91.2

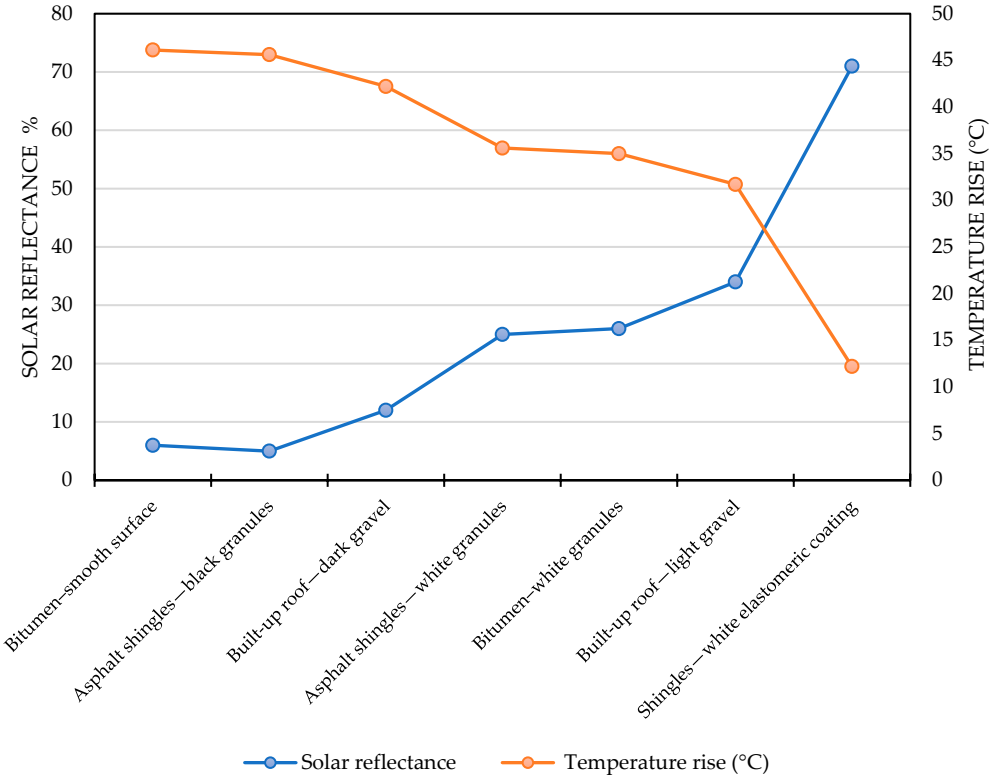

Figure 4. Correlation between roof temperature and solar reflectance in materials with the same infrared emittance range [37].

4. Surface Solar Reflectivity

Surface solar reflectivity is considered by radiative cooling and retro-reflectivity. Radiative cooling is a passive technique that cools objects by emitting thermal energy into outer space, taking advantage of the effect of night-sky radiation, a highly common means of energy transfer from the Earth's surface [38]. The universe, having a temperature close to absolute zero, acts as an ultimate heat sink and a substantial renewable thermodynamic resource. As a result, radiative cooling allows terrestrial objects to discharge heat into outer space as electromagnetic waves, providing a passive cooling mechanism that does not require additional energy input. With the growing risk of extreme heat waves due to climate change, radiative cooling has the capability to disperse excessive heat away from the Earth. [39]. However, atmospheric interference limits its efficiency, and it relies on the infrared atmospheric window (wavelengths 8 to 14 µm) for cooling where the Earth's atmosphere allows thermal radiation to pass through relatively unimpeded [38]. Two approaches are used for nighttime radiative cooling: utilizing a black body radiator and maximizing radiation within the atmospheric window. During the daytime, effective

radiative cooling requires preventing the absorption of solar radiation. Two methods are used: (I) partially transparent shielding to block undesired spectra and (II) employing a translucent material layer having a high radiation rate and high degree of solar reflectivity. The latter approach has been successfully demonstrated to provide passive cooling, even in direct sunlight [38]. Early research on radiative sky cooling primarily focused on nighttime applications due to limited cooling capacity during the day because of solar absorption [40]. Progress in materials and equipment for nighttime cooling have shown efficiencies of up to 10–15 °C below ambient temperatures. However, the limited energy density of this technology obstructs its widespread implementation, necessitating expansive surface areas to achieve substantial cooling capabilities, leading to increased expenses associated with this technology [38].

Radiative cooling resources in seven regions of China were evaluated using a radiative cooling model alongside meteorological data for those respective areas. The maximum annual cooling potential ranged from nearly 37 to 72 W/m^2. The seasonal distribution of radiative cooling resources varied, with the lowest cooling potential over all seasons. Additionally, it was shown that a practical radiative cooler with lower solar absorption and non-blackbody thermal emittance led to an average reduction of 15% in the annual net cooling power [41].

Recent advancements have made passive daytime radiative cooling (PDRC), a technology designed to reduce the temperature of surfaces and the surrounding environment during daylight hours without the need for electricity or active cooling systems, achievable by reflecting solar radiation and increasing thermal mid-infrared emittance. To achieve PDRC, a coating with high solar reflectance to the solar spectrum (0.3–2.5 μm) is necessary to prevent solar heating. This means that even during the daytime, the heat loss to outer space through the atmospheric window is significantly greater than heat gain from solar radiation, enabling passive cooling without requiring electricity. However, it is crucial to recognize that the applicability of these conditions can vary depending on different factors such as geographical location, season, microclimate, building envelope characteristics, and specific time of day [42].

The overall transmitter efficiency serves as a performance metric for broadband infrared transmitters operating at elevated temperatures. Conversely, at sub-ambient temperatures, the ratio of the transmitter's radiance efficiency in the atmospheric window to its total radiation efficiency is employed as an indicator of its cooling efficiency. In the context of building applications, the cooling performance of radiative cooling coatings on roofs is often assessed using the solar reflectance index (SRI). SRI is determined by considering solar reflectivity and the rate of infrared thermal emission, with higher SRI values denoting more efficient radiative cooling [43]. Advancements in nano-patterning techniques and designer materials are expected to provide a broader knowledge base regarding the radiative properties of different materials [44]. To achieve an improved approach for assessing and designing radiative cooling materials and devices, it is essential to eliminate the interference caused by atmospheric radiation and solar energy [45].

In addition, retro-reflectivity (RR) is another way to cool a surface. The RR definition explains how solar radiation reflects into the atmosphere without experiencing scattering. Building envelope materials are capable to incorporate such capacity [46]. These specialized materials are ingeniously designed to alter the path of incident light in a manner that redirects it precisely back toward its source (Figure 5) rather than allowing it to scatter or disperse in various directions. In essence, the term "retroreflecting" characterizes the unique ability of a material or surface to bounce radiation back to its origin, regardless of the angle at which the light strikes the surface [47]. However, the effectiveness of RR materials is notably contingent on factors such as the angle of solar radiation and the urban density [47].

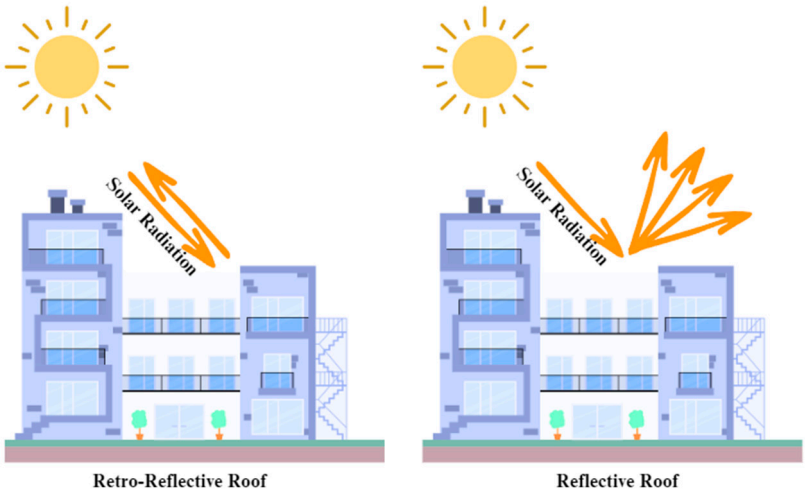

Figure 5. Retro-reflective roof reflects solar radiation back into the atmosphere in the same direction as the shortwave radiation received (**left**), vs. reflective roof that scatters solar radiation in different directions (**right**) [5].

5. Cool Building Envelope Materials

The materials that have high reflectivity and high emissivity are called cool materials. These materials can effectively reflect a fraction of the solar radiation back to the atmosphere while emitting absorbed heat through their radiative cooling ability [48]. Cool materials have three main characteristics: (I) minimal absorptivity to reduce solar heat gain; (II) radiative cooling ability by maximizing spectral emissivity to increase heat losses; and (III) high thermal capacitance and increased latent heat storage capacity to effectively regulate heat gains and lower surface temperatures. Various types of materials, such as naturally high reflective white coatings, phase change materials (PCMs), thermochromic, and fluorescent materials, offer different heat mitigation potentials and applications [49].

In the 1970s and 1980s, research mainly concentrated on the application of substances such as polyethylene, PVF, TiO_2 paint, and other coatings on aluminum substrates to generate selective surfaces that might dissipate heat effectively and perhaps result in temperature decreases, but the main challenge was to achieve radiative cooling during daytime. Progress was made through the utilization of silicon nitride films, selective infrared emissions from gases, reflective coatings, and doped polymers. These techniques occasionally resulted in temperature drops relative to the surroundings. In recent years, research has primarily focused on utilizing recycled and natural-based materials, generating power while reducing heat, and assessing the impact of varying climates and microclimates on the suitability and durability of these materials. Appendix A presents a list of key findings from studies on the utilization of cool materials.

Various cool materials, such as polymer-based porous structures and randomly distributed particle structures without a reflective metal layer, show promise for diverse commercial applications due to their impressive cooling abilities, cost-effectiveness, ease of manufacturing, scalability, and compatibility [50]. Additionally, a surface with high-potential radiative cooling utilizing a bioinspired array of truncated SiO_2 micro cones can achieve both appealing visual characteristics and efficient cooling under direct sunlight while maintaining functionality [51]. Another development involves a hierarchically structured polymethyl methacrylate (PMMA) film with micropores and random nanopores that provides highly efficient passive radiative cooling, with temperature reductions of up to 8.2 °C at night and 6.0 °C to 8.9 °C during midday [52]. However, despite the growing significance of the use of nanostructures in radiative cooling, their widespread application is hindered by high fabrication costs [44].

Efficient sub-ambient daytime radiative cooling (DRC) was achieved using a naturally derived cellulose nanocrystal (CNC) film. This film selectively reflects visible light while

maintaining low solar absorption and high mid-infrared emission, offering effective heat loss. By combining the CNC film with a scattering ethyl cellulose (EC) base layer, broad-spectrum solar reflection and vibrant structural color can be achieved simultaneously. The scalable roll-to-roll manufacturing process makes this sustainable and cost-effective approach commercially viable for large-scale production, presenting a potential solution for sub-ambient radiative cooling with implications for addressing global warming and promoting carbon neutrality [53].

A multilayered hydrophobic fabric composed of polydimethylsiloxane (PDMS), polymethyl methacrylate (PMMA), and cotton can achieve efficient passive daytime radiative cooling (PDRC). The fabric exhibits high solar reflectivity (0.94) and suitable atmospheric window emissivity (0.79), achieving temperature reductions of up to 7.8 °C under direct sunlight [54]. Magnesium-doped SiO_2 coatings demonstrated high solar reflectance of up to 86% and superior radiative cooling properties compared to pure SiO_2 coatings, achieving a maximum temperature reduction of 17.8 °C compared to empty space and 4.5 °C compared to commercial SiO_2 coatings [55].

Cooling energy savings of up to 2.9 kW h/m^2 per 0.1 increase in solar reflectance, as well as average reductions of 1.1 °C in indoor operative temperature and up to 7.5 °C on exterior surface temperatures, were calculated, highlighting cool facades as a viable technology for improving energy efficiency and environmental quality in Mediterranean dwellings [56]. The energy-saving potential of thermochromic materials in Mediterranean residential buildings was also assessed through dynamic modeling, showing improved yearly energy performance with absolute energy savings of up to 25 kWh/m^2 and relative savings of 4–19% [57]. Cool-colored materials for facades in new constructions and building renovations were assessed, including the impact of solar reflectance on cool-colored paints. Reflectance and thermal emissivity measurements were conducted for two categories of cool colors, resulting in significant surface temperature reductions and a 10–20% improvement in energy performance during the cooling season for residential buildings in different Italian climates [58]. Nanocomposite-based cool coatings, specifically the NanoDPR coating, exhibited enhanced durability and slower reduction in solar reflectance index compared to reference coatings, leading to potential average annual energy savings of 5% and a significant reduction in CO_2 emissions in extreme climates such as that experienced in the UAE [59].

Cool materials, specifically cool asphalt, can be used for pavement and roadways. It was found that cool asphalt applications resulted in average temperature differences of 3 °C to 5.5 °C compared to conventional asphalt after measuring the optical and thermal properties of asphalt samples [60]. This is because cool asphalt surfaces remain cooler under solar radiation, leading to reduced heat transfer to the surrounding air, ultimately resulting in lower temperatures [60]. Experiments were conducted on a coated pavement in a hot desert environment, showing that increasing solar reflectivity led to reduced surface temperatures, lower energy consumption, and decreased CO_2 emissions. Applying highly reflective white coatings offers multiple advantages, including mitigating the UHI effect and extending materials sustainability and durability [27]. In-depth analyses, including measurements and numerical evaluations, have yielded compelling results in favor of employing cool building envelope materials to mitigate UHI effects.

6. Solar Reflectivity Measurements of Building Envelope Materials

Measuring solar reflectivity is essential when studying the effect of cool materials because it provides crucial insights into the ability of materials to reflect solar radiation and reduce heat absorption. By accurately measuring reflectivity, one can assess the potential of cool materials in mitigating UHI effects and enhancing thermal comfort, thereby contributing to more sustainable and energy-efficient urban designs. Figure 6 shows the measuring procedure as used in cool material evaluation studies. Two parameters are measured: surface solar reflectivity and surface heat emissivity. Specific instruments and relevant standards need to be followed for measuring the reflectivity and emissivity of

building facade materials. A spectrophotometer or a reflectometer can be used to measure the reflectivity (also known as the albedo) of building facade materials. These instruments measure the amount of light reflected from a surface across different wavelengths [61].

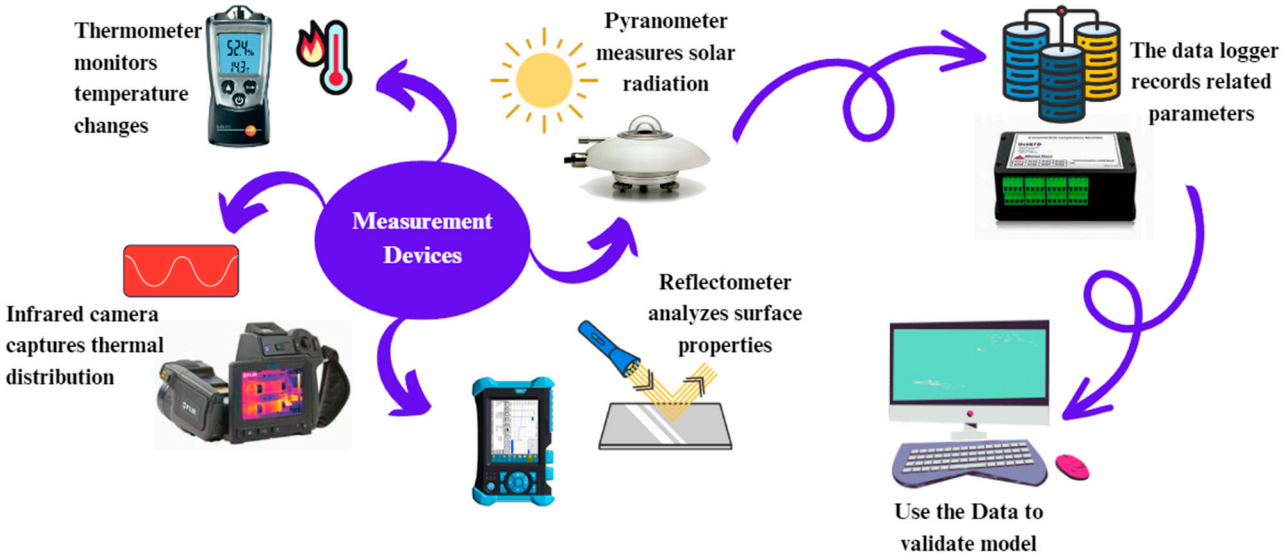

Figure 6. Experimental procedure for cool building envelope material measurements [5].

Two methods are used to measure emissivity at various temperatures: calorimetric and radiometric methods. The calorimetric method is a commonly used and straightforward approach involving three components: a radiator, a receiver, and the sample. The sample's role as either the radiator or absorber depends on the known radiative properties of the other components. By measuring the heat transfer from the radiator to the absorber, it is possible to calculate the radiative properties and the total hemispherical emissivity of the sample [62]. Radiometric methods use radiometric instruments to directly measure the radiative properties of a sample. One radiometric method is the measurement of spectral emissivity. This method utilizes Fourier transform infrared (FTIR) spectrometers to analyze the thermal radiation emitted by the sample across a range of wavelengths. By comparing the measured radiation with the known properties of a reference material, the emissivity can be calculated at different wavelengths and/or over a broad spectral range [63].

Another radiometric method is infrared (IR) thermography. In this method, an IR camera is used to capture the thermal radiation emitted by the sample. The camera detects temperature distribution on the surface of the sample and calculates emissivity based on temperature measurements. This method is particularly useful for non-contact measurements and large-area assessments of emissivity. Radiometric methods offer advantages such as direct measurements, non-contact capabilities, and the ability to obtain emissivity values across a wide range of temperatures and wavelengths. To obtain valuable results, it is crucial to take into consideration elements such as surface roughness, the surrounding environmental conditions, and the accuracy of calibration standards.

The use of radiometric techniques for temperature measurement poses two key challenges. The first challenge is the need to determine the object's emissivity, which is essential for accurately calculating its surface temperature. The second challenge involves the impact of background radiation from nearby objects and interactions with the environment, which can notably affect the radiation detected and, consequently, the temperature readings [64]. To measure the emissivity of building facade materials, an infrared (IR) camera with emissivity measurement capabilities can be utilized.

7. Numerical Simulation of Building Envelope Materials

Understanding the effects of using cool building envelope materials for mitigating UHI effects requires the integration of building energy modeling and urban/local climate/environment assessment. In essence, the energy demand of a building depends on multiple factors, encompassing the heat transfer characteristics of its envelope, ambient air and radiant temperatures, solar heat gains from both vertical and horizontal components, and the accumulation of heat within structural materials. Understanding and addressing these interrelated factors are critical in achieving effective UHI mitigation and optimizing building energy performance. These interactions between indoor and outdoor raise the need for microclimate modeling, which can integrate a building energy model (BEM) with an outdoor computational fluid dynamics (CFD) model. As such, simulation studies are categorized into two control volumes: building simulations and urban micro-climate modeling. Figure 7 shows the general approach to evaluating cool materials, consisting of experimental measuring, numerical modeling, and the evaluation and forecasting for future use of these materials in buildings and built environments. The experimental measurements are explained in the previous section.

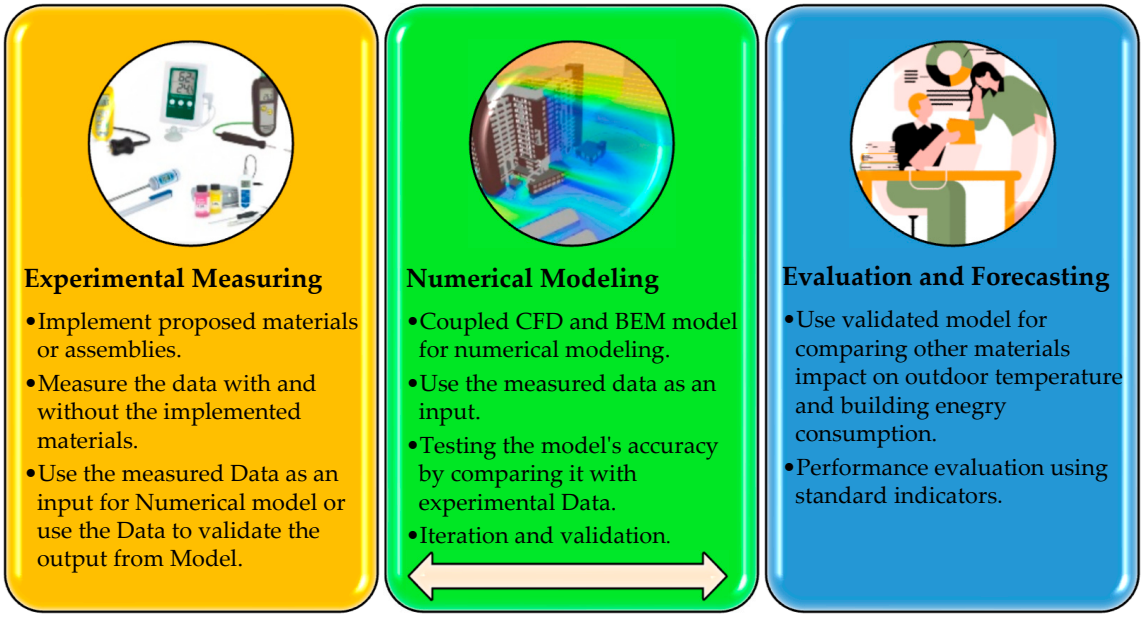

Figure 7. The general approach in evaluating cool materials performance.

7.1. Building Simulations

The integration of CFD and BEM offers a powerful tool not only for estimating outdoor environmental conditions but also for designing new buildings. By simulating the airflow patterns, heat transfer, and energy performance of buildings, the use of CFD-BEM approaches enables architects and engineers to optimize the design of structures to enhance thermal comfort and energy efficiency [65]. These approaches allow for the evaluation of various design alternatives, such as building form, orientation, and fenestration, by assessing their impact on indoor airflow, temperature distribution, and energy consumption.

The impact of cool roofs has been extensively studied, whereas research on their effects on walls or comparisons between effects from walls and roofs is limited.

Li et al. developed a prediction model using nonlinear regression to calculate the heat transfer coefficient of building walls, considering solar energy effects and wind influences in winter. The model's findings showed that the heat transfer coefficient of the walls was notably affected by the heat accumulation coefficient and the heat transfer coefficient of the south wall's outer surface on sunny days. However, the study also revealed that radiation

intensity and outdoor air temperature had minimal influence on these factors. The higher heat transfer values for walls signify better heat transfer efficiency through walls [66].

Yu et al. proposed a simulation-based method for comparing the cooling performance of different daytime radiative cooling materials. The method utilizes basic radiation theory, the standard solar spectrum, and six standard model atmospheres to evaluate and compare materials under various environmental conditions. The MODTRAN code has been used for the prediction and analysis of optical measurements through the atmosphere. By applying this method, engineers can select the most suitable radiative cooling material for specific environments. The most significant energy savings occurred in the U.S. standard atmosphere (1976) scenario among the six different standard model atmospheres in MODTRAN, which are Sub-arctic summer, Sub-arctic winter, Mid-latitude summer, Mid-latitude winter, Tropical atmosphere, and U.S. standard atmosphere [67]. Within this study, a simulation analysis was conducted to compare four materials, and it was found that one of these materials (porous poly vinylidene fluoride-co-hexafluoro propene) [68] exhibited the highest cooling power [67].

As for numerical modeling, the results derived from CFD—BEM simulations provide insights into the interaction between buildings and their surrounding microclimates, enabling the identification of strategies to mitigate the effects of other factors such as wind patterns, solar radiation, and the UHI effect. By leveraging CFD—BEM approaches, designers can make informed decisions to create buildings that not only respond to outdoor thermal conditions but also contribute to occupant comfort and the overall sustainability of the building operations.

7.2. Micro-Climate Simulations

The importance of considering building—microclimate interactions in urban planning arises due to the UHI impacts, which affect building cooling loads and are influenced by urban morphology, landscaping, and thermal properties. In a case study undertaken in La Rochelle, France, EnviBatE and SOLENE-Microclimate simulation tools were used during the design stage to compare two building densities, revealing significant reductions in wind velocity and solar irradiation on existing nearby buildings in the densified district; this permitted highlighting the ability of microclimate simulation tools [69].

Gros et al. developed the Envi-BatE model, which combines BEM with an urban canopy concept on a district scale to analyze microclimatic effects on building energy demand [70]. Cool paints, especially on vertical walls, significantly reduced cooling energy demand and improved the local microclimate [71]. A new co-simulation model was developed by Miguel et al., which combined EnergyPlus and OpenFOAM. The model accurately observes waste heat release from cooling systems and assesses direct and indirect effects for countering UHI effects. The model was validated using field experiment measurements, and it was found to approximate outdoor temperature and air motion adequately; however, improvements were needed to better estimate surface temperatures by considering net-longwave radiation when undertaking EnergyPlus building energy simulations [72].

Scaled outdoor field measurements were performed by Wang et al. using the SOMUCH experimental platform to examine the daily features of the urban thermal environment and surface energy balance (SEB) within a 3D urban configuration. The study revealed different surface and air temperatures, with direct solar radiation being the primary influencing factor. Wall temperatures were significantly affected by height and orientation in high-rise compact urban structures. Hollow samples were used, and those samples filled with water permitted the heat absorption capacity of water to be used as an indoor "situation" indicator. The water model showed lower temperature variation and a smaller diurnal temperature range compared to the hollow model, emphasizing the impact of thermal storage capacity. The study also permitted the observation of how surface albedo is affected by the solar altitude angle, sky conditions, and building aspect ratio. The findings provided valuable insights for future urban climate studies and also permitted enhancing numerical simulations of urban surface energy balance models [73].

Fallahpour et al. proposed a repeatable, step-by-step framework for outdoor thermal comfort assessment (OTC) that combined dynamic building energy simulation (BES) with CFD for external surface temperatures, microclimate CFD for wind velocity, and Honeybee software 0.0.66 for solar radiation. Although the framework was location and design-independent, it had limitations, such as considering a constant ground surface temperature in simulations that would underestimate the microclimate impact due to the low spatial resolution of building surface temperatures from the results of BES. Future improvements should incorporate dynamic CFD-based meteorological parameters to allow evaluation of the framework of larger-scale urban areas having diverse building materials and geometries [74].

Lu et al. conducted scaled outdoor experiments within 3D high-rise building clusters to explore how cool coatings affect the parameters of the urban thermal environment. Results indicated that cool coatings on both roofs and walls can increase urban albedo and reduce wall temperatures. However, cool coatings on lower-level walls were less effective in this regard. The findings highlight the potential of cooling materials in mitigating the UHI effect, suggesting their application on roofs and higher-level walls for better results [26].

7.3. Mesoscale Modeling

In mesoscale meteorological modeling, physical models, including those for radiation, the planetary boundary layer, microphysics, cumulus convection, and land surface processes, are utilized to calculate various terms of the governing equations. The weather research and forecasting (WRF) model is a numerical weather prediction system used for simulating and forecasting weather and atmospheric conditions.

To understand the impact of elevated reflectivity on urban meteorological processes and local climate and to validate simulation results with empirical measurements, it is imperative to encompass all influential factors within an integrating model framework. This entails a thorough consideration of urban canopy characteristics, including building materials, heights, and spatial layout, which exert significant influence on the local microclimate. Increasing surface reflectivity can profoundly affect the balance of solar radiation absorption and reflection, consequently shaping temperature patterns and the energy equilibrium. Furthermore, factors such as wind flow dynamics, meteorological parameters, and existing local climate conditions must be seamlessly integrated into the model to holistically assess the complex interactions occurring within the urban environment, necessitating the synergy of mesoscale and microscale models [75]. The effects of increasing urban surface albedo on the urban microclimate and building energy demand are investigated by coupling the numerical WRF model with a building effect parameterization (BEP) and BEM. The WRF model is utilized for numerical weather prediction based on real data, while the BEP predicts heat and moisture fluxes from urban canopies to the atmosphere, and the BEM simulates anthropogenic heat emissions. As a result, a comprehensive assessment is conducted, considering the various factors influencing the urban microclimate and their interactions. Microclimate outcomes, such as air temperature and wind speed, are compared with measurements taken in Toronto during the 2018 heatwave period to validate the WRF model. To evaluate potential strategies for mitigating urban heat islands, the albedos of roofs, walls, and ground surfaces are incrementally increased by 0.45, 0.4, and 0.25 from the initial 0.2, respectively, revealing a maximum air temperature reduction of nearly 2 °C at noon, along with a slight increase in wind speed [76,77]. Using the coupled WRF and UCM model, the temporal and spatial distribution of pollutants over North America was simulated during the 2011 heatwave period. The albedo of roofs, walls, and roads increased by 45%, 40%, and 25%, respectively, from their initial value of 0.2. It was observed in the simulations that in urban areas, there was a decrease of 0.7 °C in the average daily maximum air temperature [78].

Jandaghian et al. investigated the impact of urban parameterization modeling using the advanced WRF model. The WRF is integrated independently with three urban canopy models (UCMs) to predict heat and moisture exchanges between urban surfaces

and the atmosphere. Urban canopy models can be employed to simulate the dispersion of temperature, wind speed, and pollutants within a confined two-dimensional street environment [79,80]. These UCMs include a slab model (SB), a single-layer model (SL), and a multi-layer model (ML) that respectively treat buildings as roughness elements, use a simplified two-dimensional representation, and incorporate a comprehensive three-dimensional approach accounting for vertical exchange of heat, moisture, and momentum. The WRF-UCM simulations are focused on a specific heatwave period and validated by comparing the model results for air temperature, wind speed, relative humidity, and dew point temperature with observations from various weather stations [81–83]. The UCM-WRF model can be coupled with BEM to estimate the effects of increasing reflectivity on building energy consumption. Enhancing the albedo of roofs, walls, and roads to values of 0.65, 0.60, and 0.45, respectively, resulted in a 3–5% reduction in HVAC energy consumption in Toronto during the 2018 heat wave period [84].

The sensitivity of near-surface air temperature, wind speed, relative humidity, and precipitation to various physical models within the WRF model is evaluated for urban climate simulations and UHI mitigation in Montreal, Canada. A multi-layer urban canopy model is employed to account for turbulence between buildings in urban areas. The ensemble of models with the least error is recommended as a suitable platform for urban climate simulations aimed at investigating UHI mitigation strategies. Surface reflectivity is increased to mitigate the UHI effect across the region, with albedo values raised for roofs, walls, and roads. The results of surface modifications reveal a 0.2 °C decrease in averaged 2 m air temperature, a slight increase in 10 m wind speed, a 2.8% reduction in relative humidity, and an average precipitation decrease of 0.2 mm. The increased albedo results in a net reduction in radiative flux into the ground, subsequently leading to decreased convective cloud formation and precipitation [85].

WRF with a multi-layer urban canopy model (ML-UCM) can be coupled with the heat-related mortality (HRM) model. Jandaghian et al. investigated the effect of increasing the albedo of urban surfaces. Using data from the Canadian Environmental Health Atlas (CEHA), which reports an average of 120 heat-induced deaths in Toronto and Montreal, the research assesses the impact of increased surface albedo (ISA) on HRM. The results indicate that ISA results in a reduction in air temperature, a decrease in dew point temperature, and a slight increase in near-surface wind speed. This albedo increases shifts in the number of days with milder conditions by around 60%, leading to a 3–7% reduction in HRM, potentially saving seven to eighteen lives [86].

These models play a pivotal role in assessing the impact of urban development and climate change on cities, assisting in designing energy-efficient and resilient urban environments and supporting environmental policy evaluation. They provide insights into factors such as temperature variations, wind patterns, and humidity levels within urban areas, aiding in the development of strategies for mitigating UHIs, improving air quality, and enhancing the well-being of urban residents.

8. Concluding Remarks; Research Gap and Future Research Opportunities

Urban infrastructure materials, such as stone, asphalt, and concrete, substantially contribute to heat absorption and retention, exacerbating the UHI effect. In response to the negative implications of climate change and the UHI effects on buildings, occupants, and pedestrian thermal comfort, increasing solar radiation of building envelope materials is proposed. These materials, renowned for their dual attributes of high reflectivity and high emissivity, have the potential to mitigate the effects of the UHI phenomenon. Per this review, research gaps have been identified as follows:

- In comparison to studies focused only on roofs, there is still a need for more research that considers various factors such as building orientation, energy modeling for vertical surfaces, and envelope modeling, which limits understanding of their contribution to their overall potential for mitigating UHI effects. This gap necessitates more experimental and modeling studies that encompass the full range of surfaces that may be

found within urban environments. An examination of the market scenario uncovers a noticeable scarcity of information regarding the application of cool materials for external walls in North America [87]. Cool materials predominantly find use on the rooftops of non-residential structures, with a lack of available market data. Looking at the corporate landscape, a thorough investigation has identified twenty companies located in Canada, the majority of which are small and medium enterprises (SMEs) specializing in manufacturing roofing products [87]. Reflective materials, phase-change materials, and coatings are prominently featured as the most frequently discussed options in North America;

- As temperature dynamics influence wind patterns, future investigations must account for these complicated relationships to provide a more accurate picture of the potential outcomes of cool material implementation. The complex interactions between changing temperatures and wind speed, potentially leading to reduced breezes, underscore the need for comprehensive assessments that consider multiple factors;
- The absence of extensive measured data from large-scale experimental sites and long-term weather records poses a challenge in fully recognizing the implications of cool material use. Obtaining such data is essential to comprehensively evaluate their efficacy and to inform practical applications. The need for large-scale testing poses a challenge in evaluating the practical applicability of cool materials. Rigorous real-world experiments are necessary to validate the potential of these materials on a broader scale and to ensure their reliability as passive UHI mitigation strategies. Finally, the interaction between humidity and the effects of cool materials remains an area of limited understanding. Incorporating humidity-related considerations into future studies will enhance the accuracy of predictions and the overall effectiveness of cool material strategies;
- Existing cool roof measurement and rating standards, like CRRC-1 [88], only address a 3-year aging process when assessing the impact on the reflective properties of materials. Further research is needed to examine the durability of these materials under natural exposure to real field tests more comprehensively, as durability plays a vital role in the material selection process for construction purposes.

The following are the proposed research opportunities and specific steps to move forward:

- Create a comprehensive guideline that outlines the minimum prescriptive requirements for material solar reflectance index (SRI) based on the desired location. These standards can serve as a foundation for developing future building codes, making it easier to promote the widespread adoption of reflective materials and ensuring their consistent and effective use in various urban environments;
- Expand the focus beyond roofs to encompass vertical surfaces; this will promote a more complete understanding of the potential effects arising from the use of cool materials to reduce UHI effects;
- Develop a unified performance metric that allows for a direct comparison between different cool materials; the current set of performance indicators includes the Solar Reflectance Index, surface temperature, outdoor temperature, energy consumption, and glare from surfaces, whereas these performance indicators offer valuable insights, a comprehensive unit performance indicator would enable researchers, practitioners, and policymakers to effectively evaluate and rate various materials based on their overall effectiveness in mitigating the UHI effect;
- Modify existing indicators through the development of comprehensive evaluation criteria, such as surface and air temperature metrics; this would ensure a thorough understanding of how cool materials influence the urban environment; accurate and standardized measurements of these indicators would provide a clearer picture of the extent to which cool materials contribute to, and the efficacy of materials in, reducing the UHI effect and cooling the urban environment;
- Research into cool materials derived from natural sources is an ongoing endeavor within the field of material science. Future steps might involve utilizing different

arrangements of these natural cool materials in the field of building engineering. Also, studies could focus on comparing the longevity, cost-effectiveness, and impact of these cool materials on building energy consumption and outdoor temperature.

In conclusion, undertaking this review permitted informing on the significant positive outcomes that may ensue from using cool materials as a passive radiative strategy for mitigating UHI effects. By addressing the research gaps, this paper contributes to the development of sustainable and effective measures for urban heat mitigation, as well as fostering a more climate-resilient and comfortable urban environment for future generations.

Author Contributions: Writing—original draft preparation, Z.J and B.Z.; review and editing, Z.J.; B.Z., M.L., H.G. and T.M. All authors have read and agreed to the published version of the manuscript.

Funding: This research was funded by Infrastructure Canada through the Climate Resilient Built Environment (CRBE) Initiative (National Research Council Canada Project Number: A1-020250).

Data Availability Statement: Not applicable.

Acknowledgments: The authors would like to thank Infrastructure Canada and Marianne Armstrong, director of the Climate Resilient Built Environment (CRBE) Initiative, for their supports on this R&D project.

Conflicts of Interest: The authors declare no conflict of interest.

Appendix A

The following table provides an inventory of various cool materials and presents the research outcomes associated with them.

Table A1. Key findings from the utilization of cool materials for radiative cooling purposes.

No.	Cool Material	Year	Key Findings	Ref.
1	Polyethylene alcohol plastic film + evaporative Aluminum.	1974	Surfaces with selective optical properties tailored to the atmospheric window between 8–13 μm can be created by applying affordable plastic materials to a metal surface.	[89]
2	PVF + Al + Substrate.	1977	Attainable temperatures and power levels can be achieved by employing selective surfaces that align with the atmospheric window.	[90]
3	TiO_2 Paint + Al Plate.	1978	Oxides and carbonates of titanium, aluminum, calcium, and zinc are promising options for creating the needed white-black selective surface because they exhibit high reflectivity in the visible spectrum.	[91]
4	Poly Methylene film (340 mm) coated on an Aluminum base.	1979	The potential to enhance radiative cooling through the reversal of the greenhouse effect is explored, and certain experimental findings are presented.	[92]
5	SiO + the Aluminum substrate.	1981	can result in temperature variances of approximately 50 °C, with a cooling capacity of around 100 W/m^2	[93]
6	Silicon nitride film applied to aluminum substrates.	1982	An alternative method for radiative cooling involves utilizing selective infrared emission from flowing C_2H+ gas confined within an IR-transparent enclosure.	[94]
7	Foil + reflective coatings and dyes from polyethylene or ethylene copolymers + a layer of absorbent pigments.	1982	The protective cover is designed for refrigerating devices and has selective optical properties, making it reflect sunlight diffusely on one side and absorb it on the other side. The cover's reflectance on the sun-exposed side is high (above 0.6), and its transmittance in the solar spectrum is low (around 0.1).	[95]

Table A1. *Cont.*

No.	Cool Material	Year	Key Findings	Ref.
8	Reflective aluminum plate, NH3, C_2H4, C_2H_4O as gas plate.	1984	Radiative cooling can be harnessed to achieve lower temperatures, even during daylight hours.	[96]
9	The SiON film + Gas + Aluminum substrate.	1984	The combination can exhibit greater cooling capability than either of the individual gases, a significant finding for real-world applications.	[97]
10	MgO +LiF + Metal reflector.	1984	Magnesium oxide and lithium fluoride hold the potential for making radiators. By using a 1.1 mm thick layer of MgO ceramic, polished on one side and backed with a metal foil, they achieved favorable infrared optical properties. In a passive cooling test, the MgO radiator reached a temperature 22 °C lower than the surrounding air, making it 30 °C colder than a highly emissive nonselective radiator.	[98]
11	TiO_2 white and black paint.	1985	Performance evaluations were conducted using three radiative cooling systems designed with surfaces made of aluminum, white TiO_2 paint, and black paint coated with polyethylene. Comparable measurements were also taken with a fourth radiator featuring an uncovered black paint surface.	[99]
12	The Aluminum plate covers SiO_2 + SiON	1985	Silicon dioxide and silicon nitride coatings were generated through Radio Frequency sputtering of silicon in the presence of either oxygen (O_2) or nitrogen (N_2).	[100]
13	The black radiation body is covered with a ZnS polyethylene film.	1992	The foil would reduce the solar heating burden on the material beneath it to a maximum of 43 W/m^2 when the sun is directly overhead, and cooling would be effective for three hours in both the morning and evening.	[101]
14	White paint + Metal reflector.	1993	The incorporation of a $BaSO_4$ extender into the paint dispersion resulted in an improvement in the cooling performance of the paint radiators.	[102]
15	Polyethylene foils containing ZnS, ZnSe, TiO_2, ZrO_2, and ZnO pigments.	1995	The temperature was slightly higher than the surrounding environment at noon, with a heating power of roughly 7.2 W/m^2. Nevertheless, this foil demonstrated that cooling of a dark surface could be achieved for over 19 h daily in a dry region near the equator. The most effective ZnS pigments, with volume fractions reaching up to 0.15 at the surface of the black body emitter, were identified as the optimal choice.	[103]
16	SiO_2 + SiON + Al + Glass.	1995	Silicon oxynitrides are particularly well suited for high emittance inside the atmospheric window.	[104]
17	Aluminum substrate, nitrogen oxide, and silica.	1996	The efficiency of silicon oxynitride material for radiative cooling applications is improved using multilayer structures.	[105]
18	Aluminum substrate, tantalum dioxide, and tungsten.	1998	The Spectral selective radiating material can attain a stable surface temperature determined by the transition temperature of the film.	[106]
19	SiO+VWO_2+Black Substrate.	1998	The choice between overcoating and sandwiching the silver islands within a medium can have a significant effect on the system's tunability.	[106]

Table A1. *Cont.*

No.	Cool Material	Year	Key Findings	Ref.
20	Aluminum substrate and silicon dioxide.	2007	The research focused on creating Si_2N_2O nanowires through a Si nitridation process, with the addition of carbon playing a crucial role. The resulting Si_2N_2O nanowires exhibited a consistent and intense green emission at 540 nm in their photoluminescence spectrum.	[107]
21	Polyethylene foil + Aluminum foil + silicon dioxide and silicon carbide.	2010	Using a combination of SiC and SiO_2 nanoparticles, effective and cost-efficient cooling is achieved within a feasible cooling system setup.	[108]
22	TiO_2 + MgF_2	2013	The structure functions as a wide-spectrum mirror for sunlight and emits significantly in the mid-infrared range, falling within the atmospheric transparency window. This results in a net cooling power exceeding 100 W/m^2 at room temperature.	[109]
23	Polyethylene Terephthalate+ silver substrate.	2015	It has been observed to be 11 degrees Celsius cooler than a nearby commercial white cool roof. This effect is achieved using carefully selected polymers and a thin silver film, resulting in exceptional values of around 100% for both reflecting solar radiation and emitting thermal energy in the infrared spectrum, specifically between 7.9 and 13 µm wavelengths.	[110]
24	Silver substrate + amorphous silicon and silicon nitride.	2016	An average cooling of 37 °C compared to the surrounding air temperature over a 24 h day/night cycle was attained, with the most substantial cooling, reaching up to 42 °C, occurring when the experimental configuration containing the emitter is subjected to the highest levels of solar radiation.	[111]
25	Metal-methyl cone nanostructure consisting of aluminum and palladium.	2017	Over 90% of the incoming solar radiation can be effectively reflected, and the typical emissivity within the atmospheric transparency window exceeds 0.9 in most directions. It is projected that a daytime net cooling power of over 100W/m^2 will be achieved at room temperature. This cooling capacity remains effective even when accounting for substantial conduction and convection heat transfer.	[112]
26	Phosphorus + silicon cubes + Silver	2017	This approach employs common materials and manufacturing methods, making it suitable for scalable production and integration with silicon photonics. This innovation holds promise for efficient, energy-saving applications in passive cooling and thermodynamic control.	[113]
27	Polyethylene + ZnO.	2017	The TiO_2+SiO_2 coating exhibits a reflectivity of 90.7% within the solar spectrum, and its emittance in the "sky window" is 90.11%. In theory, this coating has the potential to achieve a cooling effect of around 17 °C below the surrounding temperature during nighttime and approximately 5 °C below the ambient temperature when exposed to direct sunlight.	[114]
28	SiO_2 + SiN + Al_2O_3 + TiO_2 + HfO_2 and SiO_2.	2017	Applying this photonic cooler to a solar panel can lower the cell temperature by over 5.7 °C.	[115]

Table A1. *Cont.*

No.	Cool Material	Year	Key Findings	Ref.
29	TiO_2 + Carbon particles + Substrate.	2017	By incorporating nanoparticles, the coating achieves favorable radiative properties, offering spectral selectivity for effective daytime cooling.	[112]
30	Silver + polyethylene layer +SiO_2	2017	It provides an average radiative cooling capacity exceeding 110 W/m^2 throughout a continuous 72 h cycle of day and night measurements, with the peak cooling power around noon reaching 93 W/m^2 under direct solar irradiance of over 900 W/m^2. Additionally, there was a notable increase in nighttime radiative cooling compared to daytime.	[116]
31	PDMS + Sio_2+Ag	2017	A polymer-coated fused silica mirror, which serves as a near-perfect blackbody in the mid-infrared and an excellent reflector in the solar spectrum, accomplishes radiative cooling below the surrounding air temperature both during direct sunlight (8.2 °C) and at nighttime (8.4 °C).	[117]
32	SiO_2 + TiO_2 + Alumina on a silver substrate.	2017	The addition of an Al_2O_3 film, which selectively absorbs in the 8–13 µm range while being transparent to visible and near-infrared light, can improve the effectiveness of radiative cooling within standard coating designs.	[118]
33	SiO_2+TiO_2+Al + Ag + Substrate.	2017	When exposed to a standard thermal source at 323.15 K and a wind speed of 3 $m{\cdot}s^{-1}$, it can produce a net cooling power of 363.68 W/m^2, demonstrating an 18.26% increase compared to non-radiative heat exchange (natural cooling) under identical circumstances.	[119]
34	SiC doped PDMS + Al.	2017	Utilizing available commercial polymers for selective emitters offers the promise of reducing the expenses associated with radiative cooling solutions. This configuration has the capability to deliver natural cooling of as much as 12 °C below the surrounding temperature during nighttime conditions.	[120]
35	SiO_2 + PMMA + SiO_2 + Ag + Glass.	2017	Effective radiative cooling results in a temperature drop of 3.0 °C compared to the surrounding environment, which equates to a cooling of 6.6 °C below the temperature of the bare silver (Ag) mirror.	[121]
36	SiO_2 + Al_2O_3 + Ag.	2018	Exceptional absorption efficiency exceeding 99% across the spectrum from 435 to 1520 nm while maintaining low emissivity below 20% in the mid-infrared range.	[122]
37	Meta surface + SiO_2 + Al.	2018	The meta-reflector design achieves an emittance tunability of 0.48, signifying a 30% enhancement when contrasted with the unstructured film.	[123]
38	White Glass + Ag.	2019	Emitters successfully achieved sub-ambient daytime radiative cooling effects.	[124]
39	PDMS + Al.	2019	In the laboratory and an outdoor setting, temperature decreases of 9.5 °C and 11.0 °C were observed, respectively, using the thin film thermal emitter, which exhibited an average cooling power of approximately 120 W/m^2.	[125]

Table A1. *Cont.*

No.	Cool Material	Year	Key Findings	Ref.
40	PVF + Ag.	2020	Simple structure with dual layers of PVF and Ag coating. Low-cost, scalable-manufactured, durable, and anti-staining. Experimental performance of 2 °C lower than ambient under direct sunlight.	[126]
41	LiF + Ag.	2020	A module is integrated into an RC system, serving as a thermoelectric refrigerator during the day and functioning as a thermoelectric generator during the night. The later system achieves a maximum power density of 4.78 W/m^2, enabling both daytime building cooling and nighttime power generation.	[127]
42	SiO_2 + PP + Ag + Cu + Silica aerogel pad.	2020	A temperature-regulated phase change structure (TCPCS) enhances the performance of radiative cooling systems by allowing them to adapt their cooling capacity based on the surrounding temperature. During outdoor testing, the TCPCS enables the cooler to automatically deactivate at low temperatures and activate at high temperatures. As a result, the coolers equipped with TCPCS and those without it exhibit maximum temperature differences of 9.7 °C and 19.6 °C, respectively, over the course of a full day. Additionally, a V-shaped TCPCS has been designed to serve the dual purposes of cooling during summer and heating during winter simultaneously.	[128]
43	Al_2O_3+Sapphire substrate + Ag.	2020	Al_2O_3 and SiO_2 microparticles were selected to be filter materials for RC paint. RC paint exhibits extremely low absorptivity (3.2%) and high emissivity (93.5%). RC paint had a temperature difference of 10 °C with CW paint in hot summer weather. RC paint was applied to various measurement setups compared to CW paint.	[129]
44	SiCNO + Ag + Al.	2021	The structure, featuring a 5 μm thin coating, can reduce the temperature to 6.8 °C lower than the surrounding environment due to a cooling power of 93.7 W/m^2. The evaluation of the Passive Daytime Radiative Cooling (PDRC) structure included assessments of its optical properties and reliability through extended outdoor performance tests and degradation tests conducted in various environmental conditions.	[130]
45	Cellulose acetate-based films, which are recyclable, sustainable, and bioclimatic.	2022	Daytime radiative cooling material based on TiO_2 and SiO_2 mixture coating in terms of cooling performances was compared. Results have shown a drastic sub-ambient cooling of more than 3 °C and a great reduction in the indoor temperature of the building, and a reduction in the total electricity consumption of up to 60.38%.	[131]
46	Roof + Wall + Window.	2023	A radiative cooling coating with high solar reflectivity and thermal emissivity (β = 0.98, ε = 0.97) can result in electricity savings for cooling ranging from 8.2% to 29.7% across various climate regions.	[114]

Table A1. *Cont.*

No.	Cool Material	Year	Key Findings	Ref.
47	Radiative cooling glass (RCG).	2023	RCG (Reflective Coated Glass) reduces indoor temperatures by 26.43°C compared to regular glass. It significantly improves the indoor thermal environment for rooms facing different directions, with a decrease of 45.06°C in the east and west directions and 15.05°C in the north and south directions compared to ordinary glass. The study also highlights a correlation between indoor and outdoor temperatures, where indoor temperatures rise with increasing outdoor temperatures. However, RCG's effectiveness is reduced in areas with high relative humidity.	[132]
48	Photonic radiative cooler that emits highly in the atmospheric window, randomized glass polymer metamaterial, several low-cost radiative coolers based on Aluminum.	2023	Different radiative cooling materials in diverse global climates under identical weather conditions were investigated. An active application of these materials on a highly conductive surface was simulated, calculating hourly heat gains or losses to evaluate their cooling capabilities. To implement the system practically, a threshold for the total heat needs to be determined to assess its feasibility.	[133]
49	Polar dielectric embedded polymer-based radiative cooling.	2023	The dielectric properties of dielectric particles were determined using the FPSQ model. The optical characteristics of these particles were assessed using FDTD simulation and Mie theory. The depth of electromagnetic wave attenuation in the hybrid material was calculated by considering the effective complex refractive index. Experimental validation of the proposed approach demonstrated a strong agreement between calculated emissivity and measured values. Among the various dielectric particles tested (α-SiO_2, α-Al_2O_3, TiO_2, and SiC), α-SiO_2 was identified as the most suitable material for radiative cooling.	[134]
50	Poly methyl pentene + acrylic resin mixed with SiO_2 microparticles.	2023	Radiative Cooling Paint (RCP) is prepared by adding TPX to acrylic resin mixed with SiO_2. RCP is optimized based on Mie theory combined with Monte Carlo simulation. Emissivity in 8–13 μm and reflectivity in 0.2–2.5 μm of RCP are 0.91 and 92%.	[135]
51	Recycled plastics as the foam-paper composite (FPC).	2023	The combination of highly diffusely reflective polystyrene foam particles and fiber-based printer paper results in a reflectivity of 96% in the solar spectrum, a sub-ambient cooling performance of 8.4 °C, and a maximum radiative cooling power of 90 W/m^2 during a 24 h cycle.	[136]
52	Super-hydrophobic radiative cooling emitter (SRCE) and phase change material (PCM).	2023	The SRCE (Solar Reflective Coating and Emissivity) possesses a strong ability to reflect solar radiation (0.93) and exceptional selective emission properties, with an emissivity of 0.83 within the atmospheric window and 0.49 outside it. Furthermore, the SRCE demonstrates outstanding super-hydrophobic characteristics (162.2° contact angle), along with robust mechanical properties and resistance to UV radiation. Combining phase change materials (PCM) with the SRCE shows great potential for use in a wide range of climate conditions.	[137]

References

1. Howard, L. *The Climate of London: Deduced from Meteorological Observations, Made at Different Places in the Neighbourhood of the Metropolis*; Piccadilly: London, UK, 1818.
2. Mavrogianni, A.; Davies, M.; Batty, M.; Belcher, S.E.; Bohnenstengel, S.I.; Carruthers, D.; Chalabi, Z.; Croxford, B.; Demanuele, C.; Evans, S.; et al. The comfort, energy and health implications of London's urban heat island. *Build. Serv. Eng. Res. Technol.* **2011**, *32*, 35–52. [CrossRef]
3. Davies, M.; Steadman, P.; Oreszczyn, T. Strategies for the modification of the urban climate and the consequent impact on building energy use. *Energy Policy* **2008**, *36*, 4548–4551. [CrossRef]
4. Greater London Authority. *London's Urban Heat Island: A Summary for Decision Makers*; Greater London Authority: London, UK, 2006.
5. Ashrae, A.H.F.; Atlanta, G. American Society of Heating. In *ASHRAE Handbook: Fundamentals*; ASHRAE: Peachtree Corners, GA, USA, 2021.
6. Pattacini, L. Climate and urban form. *Urban Des. Int.* **2012**, *17*, 106–114. [CrossRef]
7. Huang, Y.J.; Akbari, H.; Taha, H.; Rosenfeld, A.H. The Potential of Vegetation in Reducing Summer Cooling Loads in Residential Buildings. *J. Clim. Appl. Meteorol.* **1987**, *26*, 1103–1116. Available online: http://www.jstor.org/stable/26183503 (accessed on 1 July 2023). [CrossRef]
8. Christen, A.; Vogt, R. Energy and radiation balance of a central European city. *Int. J. Climatol.* **2004**, *24*, 1395–1421. [CrossRef]
9. Jonsson, P. Vegetation as an urban climate control in the subtropical city of Gaborone, Botswana. *Int. J. Climatol.* **2004**, *24*, 1307–1322. [CrossRef]
10. Wilmers, F. Effects of vegetation on urban climate and buildings. *Energy Build* **1990**, *15*, 507–514. [CrossRef]
11. Kolokotroni, M.; Giridharan, R. Urban heat island intensity in London: An investigation of the impact of physical characteristics on changes in outdoor air temperature during summer. *Sol. Energy* **2008**, *82*, 986–998. [CrossRef]
12. Ichinose, T.; Shimodozono, K.; Hanaki, K. Impact of anthropogenic heat on urban climate in Tokyo. *Atmos. Environ.* **1999**, *33*, 3897–3909. [CrossRef]
13. Fan, H.; Sailor, D. Modeling the impacts of anthropogenic heating on the urban climate of Philadelphia: A comparison of implementations in two PBL schemes. *Atmos. Environ.* **2005**, *39*, 73–84. [CrossRef]
14. Jandaghian, Z.; Akbari, H. The effects of increasing surface reflectivity on heat-related mortality in Greater Montreal Area, Canada. *Urban Clim.* **2018**, *25*, 135–151. [CrossRef]
15. Laouadi, A.; Bartko, M.; Gaur, A.; Lacasse, M.A. *Climate Resilience Buildings: Guideline for Management of Overheating Risk in Residential Buildings*; National Research Council Canada: Ottawa, ON, Canada, 2021.
16. Laouadi, A.; Ji, L.; Shu, C.; Wang, L.; Lacasse, M.A. Overheating Risk Analysis in Long-Term Care Homes—Development of Overheating Limit Criteria. *Buildings* **2023**, *13*, 390. [CrossRef]
17. Turhan, C.; Özbey, M.F.; Çeter, A.E.; Akkurt, G.G. A Novel Data-Driven Model for the Effect of Mood State on Thermal Sensation. *Buildings* **2023**, *13*, 1662. [CrossRef]
18. Hayes, A.T.; Jandaghian, Z.; Lacasse, M.A.; Gaur, A.; Lu, H.; Laouadi, A.; Ge, H.; Wang, L. Nature-Based Solutions (NBSs) to Mitigate Urban Heat Island (UHI) Effects in Canadian Cities. *Buildings* **2022**, *12*, 925. [CrossRef]
19. Musy, M.; Malys, L.; Inard, C. Assessment of Direct and Indirect Impacts of Vegetation on Building Comfort: A Comparative Study of Lawns, Green Walls and Green Roofs. *Procedia Environ. Sci.* **2017**, *38*, 603–610. [CrossRef]
20. Liu, S.; Wang, J.; Meng, X. Spectral properties of retro-reflective materials from experimental measurements. *Case Stud. Therm. Eng.* **2022**, *39*, 102434. [CrossRef]
21. U.S. Department of Energy. *A Practical Guide to Cool Roofs and Cool Pavements*; U.S. Department of Energy: Washington, DC, USA, 2010.
22. Liu, K. Green, reflective, and photovoltaic roofs. *Constr. Can.* **2006**, *48*, 44–54.
23. Hosseini, M.; Akbari, H. Effect of cool roofs on commercial buildings energy use in cold climates. *Energy Build.* **2016**, *114*, 143–155. [CrossRef]
24. Jandaghian, Z.; Akbari, H. The Effect of Increasing Surface Albedo on Urban Climate and Air Quality: A Detailed Study for Sacramento, Houston, and Chicago. *Climate* **2018**, *6*, 19. [CrossRef]
25. U.S. Green Building Council. . *Reference Guide for Building Design and Construction V4*; U.S. Green Building Council: Washington, DC, USA, 2013.
26. Lu, M.; Zeng, L.; Li, Q.; Hang, J.; Hua, J.; Wang, X.; Wang, W. Quantifying cooling benefits of cool roofs and walls applied in building clusters by scaled outdoor experiments. *Sustain. Cities Soc.* **2023**, *97*, 104741. [CrossRef]
27. Ghenai, C.; Rejeb, O.; Sinclair, T.; Almarzouqi, N.; Alhanaee, N.; Rossi, F. Evaluation and thermal performance of cool pavement under desert weather conditions: Surface albedo enhancement and carbon emissions offset. *Case Stud. Constr. Mater.* **2023**, *18*, e01940. [CrossRef]
28. Rosenfeld, A.H.; Akbari, H.; Romm'tv, J.J.; Pomerantz, M. Cool communities: Strategies for heat island mitigation and smog reduction. *Energy Build.* **1998**, *28*, 51–62. [CrossRef]
29. Taha, H.; Konopacki, S.; Gabersek, S. Impacts of Large-Scale Surface Modi®cations on Meteorological Conditions and Energy Use: A 10-Region Modeling Study. *Theor. Appl. Climatol.* **1999**, *62*, 175–185. [CrossRef]

30. Synnefa, A.; Santamouris, M.; Akbari, H. Estimating the effect of using cool coatings on energy loads and thermal comfort in residential buildings in various climatic conditions. *Energy Build.* **2007**, *39*, 1167–1174. [CrossRef]
31. Oleson, K.W.; Bonan, G.B.; Feddema, J. Effects of white roofs on urban temperature in a global climate model. *Geophys. Res. Lett.* **2010**, *37*, L03701. [CrossRef]
32. Gagliano, A.; Detommaso, M.; Nocera, F.; Evola, G. A multi-criteria methodology for comparing the energy and environmental behavior of cool, green and traditional roofs. *J. Affect. Disord.* **2015**, *90*, 71–81. [CrossRef]
33. Imran, H.; Kala, J.; Ng, A.; Muthukumaran, S. Effectiveness of green and cool roofs in mitigating urban heat island effects during a heatwave event in the city of Melbourne in southeast Australia. *J. Clean. Prod.* **2018**, *197*, 393–405. [CrossRef]
34. Macintyre, H.; Heaviside, C. Potential Benefits of Cool Roofs in Reducing Heat-Related Mortality during Heatwaves in a Eu-ropean City. Available online: http://lpdaac.usgs.gov (accessed on 1 July 2023).
35. Lynn, B.H.; Lynn, I.M. The impact of cool and green roofs on summertime temperatures in the cities of Jerusalem and Tel Aviv. *Sci. Total. Environ.* **2020**, *743*, 140568. [CrossRef]
36. Falasca, S.; Zinzi, M.; Ding, L.; Curci, G.; Santamouris, M. On the mitigation potential of higher urban albedo in a temperate oceanic metropolis. *Sustain. Cities Soc.* **2022**, *81*, 103850. [CrossRef]
37. Konopacki, S.; Gartland, L.; Akbari, H.; Rainer, L. *Demonstration of Energy Savings of Cool Roofs*; OSTI: Washindgton, DC, USA, 0000. [CrossRef]
38. Hu, Z.; Mu, E. *Infrared Radiative Cooling and Its Applications*; Springer Nature: Singapore, 2022. [CrossRef]
39. Johnson, T. Radiation cooling of structures with infrared transparent wind screens. *Sol. Energy* **1975**, *17*, 173–178. [CrossRef]
40. Zhao, B.; Hu, M.; Ao, X.; Chen, N.; Pei, G. Radiative cooling: A review of fundamentals, materials, applications, and prospects. *Appl. Energy* **2018**, *236*, 489–513. [CrossRef]
41. Chen, J.; Lu, L.; Gong, Q. A new study on passive radiative sky cooling resource maps of China. *Energy Convers. Manag.* **2021**, *237*, 114132. [CrossRef]
42. Chen, M.; Pang, D.; Chen, X.; Yan, H.; Yang, Y. Passive daytime radiative cooling: Fundamentals, material designs, and applications. *EcoMat* **2021**, *4*, e12153. [CrossRef]
43. Smith, G.B.; Gentle, A.R.; Arnold, M.D.; Gali, M.A.; Cortie, M.B. The importance of surface finish to energy performance. *Renew. Energy Environ. Sustain.* **2017**, *2*, 13. [CrossRef]
44. Family, R.; Mengüç, M.P. Materials for Radiative Cooling: A Review. *Procedia Environ. Sci.* **2017**, *38*, 752–759. [CrossRef]
45. Fan, F.; Xu, D.; Zhu, Y.; Tan, G.; Zhao, D. A simple, accurate, and universal method for characterizing and comparing radiative cooling materials and devices. *Int. J. Heat Mass Transf.* **2023**, *200*, 123494. [CrossRef]
46. Wang, J.; Liu, S.; Meng, X.; Gao, W.; Yuan, J. Application of retro-reflective materials in urban buildings: A comprehensive review. *Energy Build.* **2021**, *247*, 111137. [CrossRef]
47. Yuan, J.; Shimazaki, Y.; Zhang, R.; Masuko, S.; Cao, S.-J. Can retro-reflective materials replace diffuse highly reflective materials for urban buildings' wall to improve outdoor thermal comfort? *Heliyon* **2023**, *9*, e14872. [CrossRef]
48. Hendel, M. Cool pavements. In *Eco-Efficient Pavement Construction Materials*; Elsevier: Amsterdam, The Netherlands, 2020; pp. 97–125. [CrossRef]
49. Santamouris, M.; Yun, G.Y. Recent development and research priorities on cool and super cool materials to mitigate urban heat island. *Renew. Energy* **2020**, *161*, 792–807. [CrossRef]
50. Yu, X.; Chan, J.; Chen, C. Review of radiative cooling materials: Performance evaluation and design approaches. *Nano Energy* **2021**, *88*, 106259. [CrossRef]
51. Ding, Z.; Pattelli, L.; Xu, H.; Sun, W.; Li, X.; Pan, L.; Zhao, J.; Wang, C.; Zhang, X.; Song, Y.; et al. Iridescent Daytime Radiative Cooling with No Absorption Peaks in the Visible Range. *Small* **2022**, *18*, e2202400. [CrossRef] [PubMed]
52. Wang, T.; Wu, Y.; Shi, L.; Hu, X.; Chen, M.; Wu, L. A structural polymer for highly efficient all-day passive radiative cooling. *Nat. Commun.* **2021**, *12*, 365. [CrossRef] [PubMed]
53. Zhu, W.; Droguet, B.; Shen, Q.; Zhang, Y.; Parton, T.G.; Shan, X.; Parker, R.M.; De Volder, M.F.L.; Deng, T.; Vignolini, S.; et al. Structurally Colored Radiative Cooling Cellulosic Films. *Adv. Sci.* **2022**, *9*, e2202061. [CrossRef] [PubMed]
54. Ji, Y.; Sun, Y.; Muhammad, J.; Li, X.; Liu, Z.; Tu, P.; Wang, Y.; Cai, Z.; Xu, B. Fabrication of Hydrophobic Multilayered Fabric for Passive Daytime Radiative Cooling. *Macromol. Mater. Eng.* **2021**, *307*, 2100795. [CrossRef]
55. Zhang, X.; Gao, X.; Dong, Y.; Wu, Y.; Duan, D.; Zhao, X.; Li, X. Nanoporous Mg-doped SiO2 nanoparticles with tunable infrared emissivity toward effective radiative cooling coatings. *J. Alloys Compd.* **2023**, *940*, 168905. [CrossRef]
56. Zinzi, M. Exploring the potentialities of cool facades to improve the thermal response of Mediterranean residential buildings. *Sol. Energy* **2016**, *135*, 386–397. [CrossRef]
57. Zinzi, M.; Agnoli, S.; Ulpiani, G.; Mattoni, B. On the potential of switching cool roofs to optimize the thermal response of residential buildings in the Mediterranean region. *Energy Build.* **2020**, *233*, 110698. [CrossRef]
58. Zinzi, M. Characterisation and assessment of near infrared reflective paintings for building facade applications. *Energy Build.* **2016**, *114*, 206–213. [CrossRef]
59. Nutakki, T.U.K.; Kazim, W.U. Performance testing of nanocomposite based coatings with high dust pickup resistance and solar reflective index for energy efficiency in built environment. *Mater. Today Proc.* **2023**. [CrossRef]
60. Carnielo, E.; Zinzi, M. Optical and thermal characterisation of cool asphalts to mitigate urban temperatures and building cooling demand. *Build. Environ.* **2013**, *60*, 56–65. [CrossRef]

61. Surfaceoptics Measuring Instruments. Available online: https://surfaceoptics.com/products/reflectometers-emissometers/410-vis-ir/ (accessed on 1 July 2023).
62. Zhao, Y.; Li, X.; Zhang, H.; Shen, F.; Huang, C.; Liu, H.; Qi, H.; Huang, Z.; Geng, Z.; Xin, J.; et al. Preliminary development of emissivity measurement system at low temperature based on radiometric method. *Cryogenics* **2023**, *132*, 103671. [CrossRef]
63. Langsdale, M.F.; Wooster, M.; Harrison, J.J.; Koehl, M.; Hecker, C.; Hook, S.J.; Abbott, E.; Johnson, W.R.; Maturilli, A.; Poutier, L.; et al. Spectral Emissivity (SE) Measurement Uncertainties across 2.5–14 μm Derived from a Round-Robin Study Made across International Laboratories. *Remote Sens.* **2020**, *13*, 102. [CrossRef]
64. Vuelban, E.M.; Girard, F.; Battuello, M.; Nemeček, P.; Maniur, M.; Pavlásek, P.; Paans, T. Radiometric Techniques for Emissivity and Temperature Measurements for Industrial Applications. *Int. J. Thermophys.* **2015**, *36*, 1545–1568. [CrossRef]
65. Schreiber, H.; Jandaghian, Z.; Baskaran, B. Energy performance of residential roofs in Canada—Identification of missing links for future research opportunities. *Energy Build.* **2021**, *251*, 111382. [CrossRef]
66. Li, H.; Jia, H.; Zhong, K.; Zhai, Z. Analysis of factors influencing actual absorption of solar energy by building walls. *Energy* **2020**, *215*, 118988. [CrossRef]
67. Yu, X.; Chen, C. A simulation study for comparing the cooling performance of different daytime radiative cooling materials. *Sol. Energy Mater. Sol. Cells* **2020**, *209*, 110459. [CrossRef]
68. Mandal, J.; Fu, Y.; Overvig, A.C.; Jia, M.; Sun, K.; Shi, N.N.; Zhou, H.; Xiao, X.; Yu, N.; Yang, Y. Hierarchically porous polymer coatings for highly efficient passive daytime radiative cooling. *Science* **2018**, *362*, 315–319. [CrossRef]
69. Gros, A.; Bozonnet, E.; Inard, C.; Musy, M. Simulation tools to assess microclimate and building energy—A case study on the design of a new district. *Energy Build.* **2016**, *114*, 112–122. [CrossRef]
70. Gros, A.; Bozonnet, E.; Inard, C. Cool materials impact at district scale—Coupling building energy and microclimate models. *Sustain. Cities Soc.* **2014**, *13*, 254–266. [CrossRef]
71. Tsoka, S.; Tsikaloudaki, A.; Theodosiou, T. Analyzing the ENVI-met microclimate model's performance and assessing cool materials and urban vegetation applications–A review. *Sustain. Cities Soc.* **2018**, *43*, 55–76. [CrossRef]
72. Miguel, M.; Hien, W.N.; Marcel, I.; Chung, H.D.J.; Yueer, H.; Zhonqi, Y.; Ji-Yu, D.; Raghavan, S.V.; Son, N.N. A physically-based model of interactions between a building and its outdoor conditions at the urban microscale. *Energy Build.* **2021**, *237*, 110788. [CrossRef]
73. Wang, D.; Shi, Y.; Chen, G.; Zeng, L.; Hang, J.; Wang, Q. Urban thermal environment and surface energy balance in 3D high-rise compact urban models: Scaled outdoor experiments. *J. Affect. Disord.* **2021**, *205*, 108251. [CrossRef]
74. Fallahpour, M.; Aghamolaei, R.; Zhang, R.; Mirzaei, P.A. Outdoor thermal comfort in urban neighbourhoods by coupling of building energy simulation and computational fluid dynamics. *J. Affect. Disord.* **2022**, *225*, 109599. [CrossRef]
75. Berardi, U.; Jandaghian, Z.; Graham, J. Effects of greenery enhancements for the resilience to heat waves: A comparison of analysis performed through mesoscale (WRF) and microscale (Envi-met) modeling. *Sci. Total. Environ.* **2020**, *747*, 141300. [CrossRef] [PubMed]
76. Jandaghian, Z.; Berardi, U. Analysis of the cooling effects of higher albedo surfaces during heat waves coupling the Weather Research and Forecasting model with building energy models. *Energy Build.* **2019**, *207*, 109627. [CrossRef]
77. Jandaghian, Z.; Berardi, U. Heat island mitigation strategy in the greater Toronto area during the heat wave. *Energy Build.* **2020**, *207*, 109–627.
78. Jandaghian, Z.; Akbari, H. Effects of Increasing Surface Reflectivity on Urban Climate and Air Quality over North America. In Proceedings of the 4th International Conference on Building, Energy, Environment, COBEE, Melbourne, Australia, 5–9 February 2018.
79. Jandaghian, Z. Flow and Pollutant Dispersion Model in a 2D Urban Street Canyons Using Computational Fluid Dynamics. *Comput. Eng. Phys. Model.* **2018**, *1*, 83–93. [CrossRef]
80. Dorostkar, M.M.; Jandaghian, Z.; Wang, L.; Wang, L. Pollutant Dispersion in a Two-Dimensional Street Canyons Using Semi-Lagrangian (FFD) Approach and Zero Equation Turbulence Model Flow and Pollutant Dispersion in Urban Street Canyons: Semi-Lagrangian Approach with Zero Equation Turbulence Model. 2018. Available online: https://www.researchgate.net/publication/325297863 (accessed on 1 July 2023).
81. Jandaghian, Z.; Berardi, U. Comparing urban canopy models for microclimate simulations in Weather Research and Forecasting Models. *Sustain. Cities Soc.* **2020**, *55*, 102025. [CrossRef]
82. Jandaghian, Z.; Berardi, U. Proper choice of urban canopy model for climate simulations. In *Building Simulation Conference Proceedings: Proceedings of the 16th IBPSA Conference, Rome, Italy, 2–4 September 2019*; International Building Performance Simulation Association: Verona, WI, USA, 2019; pp. 3401–3405. [CrossRef]
83. Jandaghian, Z.; Berardi, U. The Coupling of the Weather Research and Forecasting Model with the Urban Canopy Models for Climate Simulations. In *Urban Microclimate Modelling for Comfort and Energy Studies*; Springer International Publishing: Cham, Switzerland, 2021; pp. 223–240. [CrossRef]
84. Zahra, J.; Umberto, B. Effects of increasing urban albedo in the Greater Toronto Area. *IOP Conf. Ser. Mater. Sci. Eng.* **2019**, *609*, 072002. [CrossRef]
85. Jandaghian, Z.; Touchaei, A.G.; Akbari, H. Sensitivity analysis of physical parameterizations in WRF for urban climate simulations and heat island mitigation in Montreal. *Urban Clim.* **2018**, *24*, 577–599. [CrossRef]

86. Jandaghian, Z.; Akbari, H. Increasing urban albedo to reduce heat-related mortality in Toronto and Montreal, Canada. *Energy Build.* **2020**, *237*, 110697. [CrossRef]
87. Boulanger, C.; Lacourse, M.; Senay, M.; Touchette, J. *Heat-Reducing Building Materials*; National Research Council of Canada: Ottawa, ON, Canada, 2023.
88. *ANSI/CRRC S100*; Standard Test Methods for Determining Radiative Properties of Materials. Cool Roof Rating Council: Portland, OR, USA, 2021.
89. Catalanotti, S.; Cuomo, V.; Piro, G.; Ruggi, D.; Silvestrini, V.; Troise, G. The radiative cooling of selective surfaces. *Sol. Energy* **1975**, *17*, 83–89. [CrossRef]
90. Bartoli, B.; Catalanotti, S.; Coluzzi, B.; Cuomo, V.; Silvestrini, V.; Troise, G. Nocturnal and diurnal performances of selective radiators. *Appl. Energy* **1977**, *3*, 267–286. [CrossRef]
91. Harrison, A.; Walton, M. Radiative cooling of TiO2 white paint. *Sol. Energy* **1978**, *20*, 185–188. [CrossRef]
92. Grenier, P. Réfrigération radiative. Effet de serre inverse. *Rev. Phys. Appl.* **1979**, *14*, 87–90. [CrossRef]
93. Granqvist, C.G.; Hjortsberg, A. Radiative cooling to low temperatures: General considerations and application to selectively emitting SiO films. *J. Appl. Phys.* **1981**, *52*, 4205–4220. [CrossRef]
94. Granqvist, C.; Hjortsberg, A.; Eriksson, T. Radiative cooling to low temperatures with selectivity IR-emitting surfaces. *Thin Solid Films* **1982**, *90*, 187–190. [CrossRef]
95. Silvestrini, V.; Peraldo, M.; Monza, E. Covering Element Screening off the Solar Radiation for the Applications in the Re-Frigeration by Radiation. U.S. Patent US4323619A, 6 April 1982.
96. Lushiku, E.; Eriksson, T.; Hjortsberg, A.; Granqvist, C. Radiative cooling to low temperatures with selectively infrared-emitting gases. *Sol. Wind. Technol.* **1984**, *1*, 115–121. [CrossRef]
97. Eriksson, T.; Lushiku, E.; Granqvist, C. Materials for radiative cooling to low temperature. *Sol. Energy Mater.* **1984**, *11*, 149–161. [CrossRef]
98. Berdahl, P. Radiative cooling with MgO and/or LiF layers. *Appl. Opt.* **1984**, *23*, 370–372. [CrossRef]
99. Kimball, B. Cooling performance and efficiency of night sky radiators. *Sol. Energy* **1985**, *34*, 19–33. [CrossRef]
100. Eriksson, T.; Jiang, S.-J.; Granqvist, C. Surface coatings for radiative cooling applications: Silicon dioxide and silicon nitride made by reactive rf-sputtering. *Sol. Energy Mater.* **1985**, *12*, 319–325. [CrossRef]
101. Nilsson, T.M.; Niklasson, G.A.; Granqvist, C.G. A solar reflecting material for radiative cooling applications: ZnS pigmented polyethylene. *Sol. Energy Mater. Sol. Cells* **1992**, *28*, 175–193. [CrossRef]
102. Orel, B.; Gunde, M.K.; Krainer, A. Radiative cooling efficiency of white pigmented paints. *Sol. Energy* **1993**, *50*, 477–482. [CrossRef]
103. Nilsson, T.M.; Niklasson, G.A. Radiative cooling during the day: Simulations and experiments on pigmented polyethylene cover foils. *Sol. Energy Mater. Sol. Cells* **1995**, *37*, 93–118. [CrossRef]
104. Diatezua, M.D.; Thiry, P.; Caudano, R. Characterization of silicon oxynitride multilayered systems for passive radiative cooling application. *Vacuum* **1995**, *46*, 1121–1124. [CrossRef]
105. Diatezua, D.M.; Thiry, P.A.; Dereux, A.; Caudano, R. Silicon oxynitride multilayers as spectrally selective material for passive radiative cooling applications. *Sol. Energy Mater. Sol. Cells* **1996**, *40*, 253–259. [CrossRef]
106. Tazawa, M.; Jin, P.; Yoshimura, K.; Miki, T.; Tanemura, S. New material design with V1−xWxO2 film for sky radiator to obtain temperature stability. *Sol. Energy* **1998**, *64*, 3–7. [CrossRef]
107. Lee, B.-T.; Paul, R.K.; Lee, K.-H.; Kim, H.-D. Synthesis of Si_2N_2O nanowires in porous Si_2N_2O–Si_3N_4 substrate using Si powder. *J. Mater. Res.* **2007**, *22*, 615–620. [CrossRef]
108. Gentle, A.R.; Smith, G.B. Radiative Heat Pumping from the Earth Using Surface Phonon Resonant Nanoparticles. *Nano Lett.* **2010**, *10*, 373–379. [CrossRef]
109. Rephaeli, E.; Raman, A.; Fan, S. Ultrabroadband Photonic Structures To Achieve High-Performance Daytime Radiative Cooling. *Nano Lett.* **2013**, *13*, 1457–1461. [CrossRef]
110. Gentle, A.R.; Smith, G.B. A Subambient Open Roof Surface under the Mid-Summer Sun. *Adv. Sci.* **2015**, *2*, 1500119. [CrossRef]
111. Chen, Z.; Zhu, L.; Raman, A.; Fan, S. Radiative cooling to deep sub-freezing temperatures through a 24-h day–night cycle. *Nat. Commun.* **2016**, *7*, 13729. [CrossRef]
112. Huang, Z.; Ruan, X. Nanoparticle embedded double-layer coating for daytime radiative cooling. *Int. J. Heat Mass Transf.* **2017**, *104*, 890–896. [CrossRef]
113. Zou, C.; Ren, G.; Hossain, M.; Nirantar, S.; Withayachumnankul, W.; Ahmed, T.; Bhaskaran, M.; Sriram, S.; Gu, M.; Fumeaux, C. Metal-Loaded Dielectric Resonator Metasurfaces for Radiative Cooling. *Adv. Opt. Mater.* **2017**, *5*, 1700460. [CrossRef]
114. Bao, H.; Yan, C.; Wang, B.; Fang, X.; Zhao, C.; Ruan, X. Double-layer nanoparticle-based coatings for efficient terrestrial radiative cooling. *Sol. Energy Mater. Sol. Cells* **2017**, *168*, 78–84. [CrossRef]
115. Li, W.; Shi, Y.; Chen, K.; Zhu, L.; Fan, S. A Comprehensive Photonic Approach for Solar Cell Cooling. *ACS Photonics* **2017**, *4*, 774–782. [CrossRef]
116. Zhai, Y.; Ma, Y.; David, S.N.; Zhao, D.; Lou, R.; Tan, G.; Yang, R.; Yin, X. Scalable-manufactured randomized glass-polymer hybrid metamaterial for daytime radiative cooling. *Science* **2017**, *355*, 1062–1066. [CrossRef]
117. Kou, J.-L.; Jurado, Z.; Chen, Z.; Fan, S.; Minnich, A.J. Daytime Radiative Cooling Using Near-Black Infrared Emitters. *ACS Photonics* **2017**, *4*, 626–630. [CrossRef]

118. Kecebas, M.A.; Menguc, M.P.; Kosar, A.; Sendur, K. Passive radiative cooling design with broadband optical thin-film filters. *J. Quant. Spectrosc. Radiat. Transf.* **2017**, *198*, 179–186. [CrossRef]
119. Wu, J.-Y.; Gong, Y.-Z.; Huang, P.-R.; Ma, G.-J.; Dai, Q.-F. Diurnal cooling for continuous thermal sources under direct subtropical sunlight produced by quasi-Cantor structure. *Chin. Phys. B* **2017**, *26*, 104201. [CrossRef]
120. Czapla, B.; Srinivasan, A.; Yin, Q.; Narayanaswamy, A. Potential for Passive Radiative Cooling by PDMS Selective Emitters. In *Aerospace Heat Transfer; Computational Heat Transfer; Education; Environmental Heat Transfer; Fire and Combustion Systems; Gas Turbine Heat Transfer; Heat Transfer in Electronic Equipment; Heat Transfer in Energy Systems*; American Society of Mechanical Engineers: New York, NY, USA, 2017; Volume 1. [CrossRef]
121. Suichi, T.; Ishikawa, A.; Hayashi, Y.; Tsuruta, K. Structure optimization of metallodielectric multilayer for high-efficiency daytime radiative cooling. In *Thermal Radiation Management for Energy Applications*; Al-Jassim, M.M., Bermel, P., Eds.; SPIE: Bellingham, WA, USA, 2017; p. 13. [CrossRef]
122. Wu, D.; Liu, Y.; Xu, Z.; Yu, Z.; Yu, L.; Chen, L.; Liu, C.; Li, R.; Ma, R.; Zhang, J.; et al. Numerical Study of the Wide-angle Polarization-Independent Ultra-Broadband Efficient Selective Solar Absorber in the Entire Solar Spectrum. *Sol. RRL* **2017**, *1*, 1700049. [CrossRef]
123. Sun, K.; Riedel, C.A.; Urbani, A.; Simeoni, M.; Mengali, S.; Zalkovskij, M.; Bilenberg, B.; de Groot, C.; Muskens, O.L. VO_2 Thermochromic Metamaterial-Based Smart Optical Solar Reflector. *ACS Photonics* **2018**, *5*, 2280–2286. [CrossRef]
124. Ao, X.; Hu, M.; Zhao, B.; Chen, N.; Pei, G.; Zou, C. Preliminary experimental study of a specular and a diffuse surface for daytime radiative cooling. *Sol. Energy Mater. Sol. Cells* **2018**, *191*, 290–296. [CrossRef]
125. Zhou, L.; Song, H.; Liang, J.; Singer, M.; Zhou, M.; Stegenburgs, E.; Zhang, N.; Xu, C.; Ng, T.; Yu, Z.; et al. A polydimethylsiloxane-coated metal structure for all-day radiative cooling. *Nat. Sustain.* **2019**, *2*, 718–724. [CrossRef]
126. Meng, S.; Long, L.; Wu, Z.; Denisuk, N.; Yang, Y.; Wang, L.; Cao, F.; Zhu, Y. Scalable dual-layer film with broadband infrared emission for sub-ambient daytime radiative cooling. *Sol. Energy Mater. Sol. Cells* **2020**, *208*, 110393. [CrossRef]
127. Liao, T.; Xu, Q.; Dai, Y.; Cheng, C.; He, Q.; Ni, M. Radiative cooling-assisted thermoelectric refrigeration and power systems: Coupling properties and parametric optimization. *Energy* **2021**, *242*, 122546. [CrossRef]
128. Xia, Z.; Fang, Z.; Zhang, Z.; Shi, K.; Meng, Z. Easy Way to Achieve Self-Adaptive Cooling of Passive Radiative Materials. *ACS Appl. Mater. Interfaces* **2020**, *12*, 27241–27248. [CrossRef]
129. Chae, D.; Son, S.; Liu, Y.; Lim, H.; Lee, H. High-Performance Daytime Radiative Cooler and Near-Ideal Selective Emitter Enabled by Transparent Sapphire Substrate. *Adv. Sci.* **2020**, *7*, 2001577. [CrossRef]
130. Sun, K.; Riedel, C.A.; Wang, Y.; Urbani, A.; Simeoni, M.; Mengali, S.; Zalkovskij, M.; Bilenberg, B.; de Groot, C.H.; Muskens, O.L. Metasurface Optical Solar Reflectors Using AZO Transparent Conducting Oxides for Radiative Cooling of Spacecraft. *ACS Photonics* **2017**, *5*, 495–501. [CrossRef]
131. Benmoussa, Y.; Ezziani, M.; Djire, A.-F.; Amine, Z.; Khaldoun, A.; Limami, H. Simulation of an energy-efficient cool roof with cellulose-based daytime radiative cooling material. *Mater. Today Proc.* **2023**, *72*, 3632–3637. [CrossRef]
132. Tang, Y.; Tao, Q.; Chen, Y.; Zheng, J.; Min, Y. Building envelopes with radiative cooling materials: A model for indoor thermal environment assessment based on climate adaptation. *J. Build. Eng.* **2023**, *74*, 106869. [CrossRef]
133. Carlosena, L.; Ruiz-Pardo, Á.; Rodríguez-Jara, E.Á.; Santamouris, M. Worldwide potential of emissive materials based radiative cooling technologies to mitigate urban overheating. *Build. Environ.* **2023**, *243*, 110694. [CrossRef]
134. Wu, B.; Zhang, K.; Ye, P.; Niu, Z.; Song, G. Effect of electronic and phonon properties on polar dielectric embedded polymer-based radiative cooling materials. *Sol. Energy Mater. Sol. Cells* **2023**, *260*, 112473. [CrossRef]
135. Jiang, K.; Zhang, K.; Shi, Z.; Li, H.; Wu, B.; Mahian, O.; Zhu, Y. Experimental and numerical study on the potential of a new radiative cooling paint boosted by SiO2 microparticles for energy saving. *Energy* **2023**, *283*, 128473. [CrossRef]
136. Liu, Y.; Liu, X.; Chen, F.; Tian, Y.; Caratenuto, A.; Mu, Y.; Cui, S.; Minus, M.; Zheng, Y. Eco-friendly passive radiative cooling using recycled packaging plastics. *Mater. Today Sustain.* **2023**, *23*, 100448. [CrossRef]
137. Tao, S.; Wan, Q.; Xu, Y.; Gao, D.; Fang, Z.; Ni, Y.; Fang, L.; Lu, C.; Xu, Z. Incorporation form-stable phase change material with passive radiative cooling emitter for thermal regulation. *Energy Build.* **2023**, *288*, 113031. [CrossRef]